The *Myb* family genes in the rice pathogen *Magnaporthe oryzae*: Finding and deleting more family members involved in pathogenicity.

Ya Li[1]*, Xiuxia Zheng[1], Mengtian Pei[1], Mengting Chen[1], Shengnan Zhang[1], Chenyu Liang[1], Luyao Gao[1], Pin Huang[1], Stefan Olsson[1,2]*

[1]State Key Laboratory of Ecological Pest Control for Fujian and Taiwan Crops, College of Plant Protection, Fujian Agriculture and Forestry University, Fuzhou 350002, China

[2]Plant Immunity Center, Haixia Institute of Science and Technology, College of Life Science, Fujian Agriculture and Forestry University, Fuzhou 350002, China

*Correspondence:
Ya Li and Stefan Olsson
liya-81@163.com & Stefan@olssonstefan.com

Running title: Function of Myb family genes in *Magnaporthe oryzae*

Keywords: *Magnaporthe oryzae*; Myb; transcription factors; gene deletion; functional characterization

ABSTRACT

Proteins with DNA binding Myb domains have been suggested in regulating development and stress responses. *Magnaporthe oryzae* is considered the most destructive pathogen of rice. We screened the genome for genes with Myb domains encoding since these can be needed for pathogenesis. We found *Myb1-19*. Only MoMyb1 was previously shown to be involved in pathogenesis. We succeeded in deleting 12 of the other 18 genes. MoMyb2 deletion affected mainly growth, while MoMyb13 or MoMyb15 deletions gave additional defects in conidiation and plant infection. However, RT-qPCR showed that none of the 19 Myb genes are negligibly expressed. Instead, they have different expression profiles hours post-infection when infecting rice plants. Considering this, the unchanged infection phenotype for 9 gene deletions surprised us, and we extended the analysis to expression co-regulation of all 19 Myb proteins and found 5 co-regulated groups of predicted Myb-domain proteins. MoMyb13 or MoMyb15 are discussed and motivated as candidates for further, more detailed studies with aims also outside of plant pathology. Referring to what is found in other eukaryotes, we finally discuss possible redundancy or compensatory regulations for many of the other Myb genes hiding or compensating for the effect of many complete deletions.

IMPORTANCE

Magnaporthe oryzae is considered the most important rice pathogen limiting rice production. Our study attempts to find all genes encoding a DNA-binding gene family called Myb, and we found 19, many of which have not been studied before. The Myb gene family is suspected to regulate stress responses the pathogen needs to overcome plant defenses. Inhibiting or disturbing these genes, if they are indeed regulatory, can open new ways of controlling the pathogen and learning more about its physiology and ecology.

INTRODUCTION

Rice blast disease, caused by *Magnaporthe oryzae,* is one of the most destructive diseases on rice worldwide. Each year, this disease leads to estimated economic damage of $66 billion, which is enough to feed 60 million people (Pennisi, 2010). The disease initiates from the *M. oryzae* conidia contacting to rice surface, then the conidia germinate and develop a structure called appressoria for host penetration. The mature appressoria accumulate high internal turgor pressure (Howard et al., 1991) and mechanically penetrate rice cells by forming a hyphal penetration peg (Kankanala et al., 2007). Once completing colonization, multiple infection hyphae expand intra- and intercellularly in rice tissue, and the typical blast lesions appear in 3 to 5 days (Sakulkoo et al., 2018). New conidia are produced from lesions and released to start new infection cycles. Besides attacking rice, *M. oryzae* can infect wheat, barley, finger millet, and foxtail millet (Gladieux et al., 2018). Recently, this fungus caused a wheat blast outbreak in Bangladesh, resulting in huge losses (Islam et al., 2016; Malaker et al., 2016). Given the economic importance, genetic tractability, and genome sequence availability, *M. oryzae* has become a model to study the fungal pathogenesis and interaction with host plants (Dean et al., 2005; Ebbole, 2007). Understanding the transcription-factor-mediated cellular or biological processes of *M. oryzae* is beneficial to develop novel and practical strategies to control the blast disease and ensure global food security.

Based on the similarity of the DNA-binding domain, transcription factors are categorized into up to 61 families, including bZIP, bHLH, C2H2 zinc finger, homeobox, Zn2Cys6, Myb, etc. (Verma et al., 2017). The Myb domain family of proteins is one of the largest and most diverse families containing transcription factors. A highly conserved Myb DNA-binding domain characterizes these proteins (Ambawat et al., 2013; Du et al., 2009; Prouse and Campbell, 2012; Roy, 2016; Verma et al., 2017; L., Wang et al., 2018; X., Wang et al., 2018). The Myb domain generally consists of 1 to 3 imperfect amino acid repeats; each repeat contains 50 to 53 amino acids and spatially constitutes a helix turn helix structure. The name Myb domain was acquired from v-Myb, the oncogenic motif of avian myeloblastosis virus (AMV), where it was first discovered (X., Wang et al., 2018). The Myb family is present in all eukaryotes and could thus have more than 1 billion years of evolutionary history (Eme et al., 2017). In plants, the Myb family proteins are mainly considered as transcription factors or repressors (Allan and Espley, 2018; Ambawat et al., 2013; Baldoni et al., 2015; Cao et al., 2020; Dong et al., 2015; Du et al., 2009; Dubos et al., 2010; Kim et al., 2014; Li et al., 2019; Li et al., 2019; Lin et al., 2011; Lin et al., 2012; Liu et al., 2015; Ma and Constabel, 2019; Mateos et al., 2006; Matheis et al., 2017; Mitra, 2018; Pattabiraman and Gonda, 2013; Prouse and Campbell, 2012; Roy, 2016; Valsecchi et al., 2017; Verma et al., 2017; X., Wang, et al., 2018; Wieser and Adams, 1995). However, proteins that are not classical transcription factors can contain Myb-type DNA binding domains (Hogues et al., 2008; Ma and Constabel, 2019; Mukherjee et al., 2012; Pattabiraman and Gonda, 2013; Ramos-Sáenz et al., 2019; Rodríguez-Sánchez et al., 2011; Roy, 2016; X., Wang et al., 2018; Yu et al., 2010). The Myb family does not have many members comprising 4 to 5 proteins in animal genomes (Prouse and Campbell, 2012). While in plants, the Myb family has expanded to 100 to 200 members (Prouse and Campbell, 2012). The fungal Myb family size is smaller than in plants but more extensive than in animals, with 10 to 50 members per genome (Verma et al., 2017). Animal Myb proteins are reported to regulate cell division and a discrete subset of cellular differentiation events (X., Wang et al., 2018). Plant Myb proteins bind DNA and regulate many

metabolic, cellular, and developmental processes as transcription factors or in other ways (Prouse and Campbell, 2012; Roy, 2016). Fungal DNA-binding proteins of the Myb family have been implicated to be essential for regulation to withstand stresses (Verma et al., 2017; L., Wang et al., 2018). They should consequently play a role in the pathogenicity of plant pathogens (Verma et al., 2017), especially during the entry to, and in, the necrotrophic phase of fungal plant pathogens starting as biotrophs, like *M. oryzae* when the plant starts to detect the intruding fungus and actively counteract it by innate immune responses producing ROS and toxic metabolites (Cao et al., 2022). In *M. oryzae,* 13 Myb family genes have previously been identified (Verma et al., 2017). We searched for more to investigate if any of them in in addition to Myb1 and Myb8 (Dong et al., 2015; Lee et al., 2021) singly have critical roles in regulating the pathogenicity of *M. oryzae* on rice since Myb proteins seems essential for managing fungal stress (Verma et al., 2017; L., Wang et al., 2018) characteristic of plant infection.

First, we searched for the Myb-like domains in annotated *M. oryzae*-proteins. We found 19 genes encoding for proteins containing Myb DNA binding domains, including *Myb1*, previously proven to be involved in pathogenicity (Dong et al., 2015). We attempted to delete all the remaining 18 genes except Myb1 and succeeded in deleting 12 genes. Only 2 of the 12 genes we deleted strongly affected pathogenicity when deleted singly, although all 19 identified Myb domain genes were relatively highly expressed *in planta* during different stages of infection. One of the 2 genes affecting pathogenicity is regulating melanin biosynthesis. Therefore, the lack of standard panel phenotypic effect of the deletions of many of the Myb-domain genes highly expressed during plant infection is discussed.

RESULTS

1. Myb family domain protein identification in *M. oryzae* and analysis of their amino acid similarity

Genes for 19 *Myb* family DNA binding proteins were predicted in *M. oryzae* by the Fungal Transcription Factor Database (FTFD, http://ftfd.snu.ac.kr/index.php?a=view). One gene was previously reported as MoMyb1 (Dong et al., 2015), and 9 more recently identified as *MoMyb2-10* (Lee et al., 2021) while we were writing up this work. The other 9 we named *MoMyb11* to *19* in this study (**Fig. 1A** and **B**). Protein size and domain structure analysis showed that the 19 MoMyb protein sizes vary from the maximum 2305 aa to the minimum 250 aa. Each protein consists of at least 1 Myb domain and up to 3 (**Fig. 1A**). According to amino acid sequence similarities, the 19 *M. oryzae* Myb domain-containing proteins cluster into four main groups that could have different functions (**Fig. 1B**). To investigate some of the possible biological functions of MoMyb-proteins and especially if some of the Myb proteins, other than MoMyb1 and MoMyb8 (Dong et al., 2015; Lee et al., 2021), that has been shown to be involved in the pathogenesis of rice in *M. oryzae*, 12 Myb gene deletion mutants (*Δmomyb2, 3, 4, 5, 6, 8, 9, 10, 13, 15, 16, and 18*) were generated and confirmed by Southern blot (**Fig S1**). Mutants of 5 other *Myb* genes (*MoMyb7, 11, 12, 17, 19*) could not be obtained, even when screened from more than 200 transformants of each gene containing the gene fragment that potentially can replace the target gene. *MoMyb7* has been deleted before (Lee et al., 2021) but is not involved in pathogeneses. Even if we could not achieve a mutation for this one, our lack of mutations indicates that *MoMyb17, 19, 11, and 12* could be essential genes.

135
136 **2. MoMyb2, 13, and 15 are involved in regulating *M. oryzae* growth**
137 A growth assay was performed by growing the mutants on three types of media, including
138 complete medium (CM), minimal medium (MM), and rice bran medium (RBM), for ten days to test
139 whether the respective Myb-proteins, affect *M. oryzae* radial growth. We found 3 MoMyb mutants
140 lacking proteins MoMyb2, 13, and 15 (*⊿momyb2-101, ⊿momyb13-11*, and *⊿momyb15-7*) that
141 showed significantly decreased colony size on all three media as compared to the background
142 isolate Ku80 and the corresponding gene complementary strains (*⊿momyb2-101/MoMyb2,*
143 *⊿momyb13-11/MoMyb13*, and *⊿momyb15-7/MoMyb15*) (**Fig. 2A and B**). In contrast, the other 9
144 Myb mutants showed the same colony size as the Ku80 strain (**Fig. S2**), suggesting that MoMyb2,
145 13, and 15 directly or indirectly regulate some aspects of *M. oryzae* growth. The growth inhibition
146 rate of these three mutants on different media was also calculated. The result showed that the
147 mutants show different growth inhibition effects on different media. *⊿momyb13-11* showed the
148 highest inhibition on RBM, followed by MM and CK; *Δmomyb2-101* showed the highest inhibition
149 on CM, followed by MM and RBM; *⊿momyb15-7* showed the highest inhibition on MM, followed
150 by CM and RBM (**Fig. 2C**). These results suggest that the different nutrients of these media exerted
151 different stresses on these 3 Myb mutants.
152
153 **3. MoMyb13 and 15 appear to be involved in *M. oryzae* pathogenicity in rice**
154 We tested the 12 *Myb* gene mutations we had achieved for pathogenicity on rice leaves using
155 inoculation with mycelia on agar blocks since none of the *⊿momyb13* and *⊿momyb15* that affected
156 growth formed conidia (see below). Only *⊿momyb13* and Δmomyb15 had reduced pathogenicity
157 when agar block inoculation was performed on both intact or wounded barley and rice leaves, and
158 complementations with their respective gene restored pathogenicity (**Fig. 3A-D**). Conidia
159 inoculation could not be used for these two mutants since no conidia were formed, as seen in a
160 conidiation assay (**Fig. 4A and B**). The lack of pathogenicity does not appear to result from a lack
161 of appressoria formed by the mycelial inoculum since appressoria were formed (**Fig. 3E**). There
162 were no effects on pathogenicity for the other mutants of the remaining 10 *MoMyb* genes we
163 managed to delete. Those had all typical conidia that could be used for the pathogenicity assay
164 (**Fig. S3**).
165
166 **4. MoMyb13 and MoMyb15 are involved in conidiation, and MoMyb13 regulates hydrophobins**
167 Since conidia formation is essential for the fungus to spread rice blast disease from plant to plant,
168 conidiation was more closely investigated. A conidia induction assay was performed on CM and
169 RBM media to analyze the function of Myb proteins in *M. oryzae* conidiation. Conidia was also now
170 absent for both mutants, and their respective complementation completely restored conidiation
171 showing that both MoMyb13 and MoMyb15 are indeed necessary for conidiation, at least on these
172 traditional growth media (**Fig. 4A** and **B**)**.** Small hydrophobic proteins cover aerial mycelia of many
173 ascomycetes, so-called hydrophobins, making aerial hyphae, including conidiophores, hydrophobic
174 (Bayry et al., 2012; Berger and Sallada, 2019). We had noticed that the *Δmomyb13* had a more
175 wettable mycelium (**Fig. 5A**) indicative of a lack of hydrophobins and thus decided to test if any
176 described hydrophobin genes are downregulated in the *Δmomyb13* strain as these are not affected
177 by direct regulation by MoMyb1 even if wettability was affected (Lee et al., 2021). Hydrophobin
178 *MPG1* involved in pathogenesis (Beckerman, 1996) and affect wettability was downregulated in

179 *Δmomyb13* (**Fig. 5B**). Artificial upregulation of *MPG1* in *Δmomyb13* (**Fig. 5C**) could not restore the
180 original pathogenicity (**Fig. 5D**), indicating that MoMyb13 regulates more than hydrophobins
181 necessary for successful conidia production and infection of rice.
182
183 **5. Sensitivity of Momyb13, Momyb2, and Momyb15 mutants to different stresses**
184 A standard panel of stress treatments tested whether the MoMyb mutants affected growth rates
185 on different stressing media (Li et al., 2014). A complete medium (CM) without additions was used
186 as the control medium. The MoMyb13 mutant was inhibited by SDA, strongly inhibited by CR and
187 H_2O_2 but stimulated by NaCl and SOR **(Fig. 6A and B)**. That can result from a weakened cell wall
188 with less melanization (melanin is an antioxidant) combined with lower membrane permeability
189 and higher activity of efflux pumps as compensation for these cell wall weaknesses in the mutant.
190 MoMyb15 mutants are very inhibited by SDS affecting membrane integrity but also by NaCl **(Fig.**
191 **6A and B)** which suggest that membrane pumps depending on the membrane potential might not
192 be necessarily upregulated and working in the mutant (Gostinčar et al., 2011). Loss of Myb2 mainly
193 resulted in lower inhibition than the WT especially for CR suggesting that MoMyb2 is less important
194 as stress regulator while MoMyb5 only showed increased inhibition for the SDS treatment leading
195 to membrane disruptions. The results suggest that both MoMyb13 and MoMyb15 directly or
196 indirectly regulate genes for proteins that strengthen the cell wall and cell membrane barrier in
197 several ways important for growth inside a plant and might explain why deletion of these two genes
198 lowered the pathogenicity of the fungus.
199
200 **6. MoMyb-GFP accumulates in the nucleus**
201 All the 18 newly identified Myb-protein-encoding genes were expressed as *GFP*-containing fusion
202 constructs, and the localization of these MoMyb protein GFP-fusions was investigated. It was
203 confirmed that for all putative Myb protein fusions, we got a strong enough GFP signal to visualize
204 through confocal microscopy; they accumulate to nucleus-like structures (**Fig. 7A-C** and **S4**). The
205 three genes that showed at least some changed deletion phenotypes were investigated in more
206 detail (**Fig. 7A-C)** in a Histone1-RFP background to label the nucleus in a different color (Zhang et
207 al., 2019). It then became evident that the relatively small green "dots" of the MoMyb2-GFP
208 indicate a localization to the nucleolus, where no other of the MoMybs seems to accumulate (**Fig.**
209 **7A-C** and **S4**).
210
211 **7. Expression of all identified *MoMyb* genes during infection.**
212 All *MoMyb* genes (1-19) were investigated for expression during different HPI, *in vitro* (MY), and in
213 conidia using RT-qPCR. The analysis focuses on the genes' HPI expression profiles and makes them
214 comparable and was used to make a PCA analysis of correlations of profiles. A minimum spanning
215 tree almost equivalent to clustering is also shown in the resulting PCA plot (**Fig. S5**). The Minimum
216 spanning tree is similar to a more conventional cluster plot using neighbor-joining clustering of the
217 same data (Gower similarity index and final branch as root) (**Fig. 8**). The similarities between
218 profiles can also be seen in a table containing expression profiles for each gene (**Table S2**) and
219 agrees well with blast similarities (**Table S3**). The latter suggests that similar proteins have similar
220 expression profiles.
221
222 MoMyb2 and 15 appear to have essential roles in the necrotrophic stage and in vitro. On the other

223 hand, MoMyb13 appears to be upregulated and used during the early pre-biotrophic stage (8h) of
224 plant contact, indicating that it could be a regulator of penetration and establishment in the plant.
225
226 *MoMyb8* is, in our data, upregulated in the early phase and has one peak in the later phases. It
227 seems to be involved in responses to light (Lee et al., 2021). *MoMyb1* has previously been shown
228 to be essential for infection (Dong et al., 2015), and in our data, it belongs to the regulatory cluster
229 upregulated at 8 HPI. Since we could not find growth or infection phenotypes for more than 3
230 MoMyb proteins encoded by the newly identified genes, it was expected that some of the *MoMyb*
231 genes were not expressed during plant infection at all or pseudogenes, but it turned out that all
232 genes were well expressed and expressed in planta during at different HPIs (**Fig. 8**).
233

234 DISCUSSION

235
236 The 19 genes predicted to encode Myb domain-containing proteins in *M. oryzae* (MoMyb1-19)
237 found in the Fungal Transcription Factor Database (FTFD) encodes proteins with very different sizes
238 and content of other domains (**Fig. 1A**). Thus, the Myb domain-containing genes are expected to
239 have diverse functions (Hogues *et al.*, 2008; Yu *et al.*, 2010; Rodríguez-Sánchez *et al.*, 2011;
240 Mukherjee *et al.*, 2012; Pattabiraman and Gonda, 2013; Roy, 2016; X. Wang *et al.*, 2018; Ma and
241 Constabel, 2019; Ramos-Sáenz *et al.*, 2019), and might not all be traditional transcription factors.
242 The latter is often implied for plant Myb proteins (Allan and Espley, 2018; Ambawat et al., 2013;
243 Baldoni et al., 2015; Cao et al., 2020; Dong et al., 2015; Du et al., 2009; Dubos et al., 2010; Kim et
244 al., 2014; Li et al., 2019; Li et al., 2019; Lin et al., 2011; Lin et al., 2012; Liu et al., 2015; Ma and
245 Constabel, 2019; Mateos et al., 2006; Matheis et al., 2017; Mitra, 2018; Pattabiraman and Gonda,
246 2013; Prouse and Campbell, 2012; Roy, 2016; Valsecchi et al., 2017; Verma et al., 2017; X., Wang
247 et al., 2018; Wieser and Adams, 1995). We found 6 more Myb-domain protein-encoding genes
248 than the 13 *MoMyb* genes identified earlier (Verma et al., 2017) and 9 more than were recently
249 identified (Lee et al., 2021). Interestingly, all 19 MoMyb-protein-encoding genes are expressed at
250 different stages of plant infection (**Fig. 8, S5,** and **Table S2**). Thus, it surprised us that the successful
251 only the deletion of two of our deleted genes (*Δmomyb13* and *ΔmoMyb15*) and one previously
252 deleted gene with a known effect on the infection (*Δmomyb1*) had notable effects on plant
253 infection (**Fig. 3, S3** and **Table1**). There are many possible explanations for this. One explanation is
254 that these deleted genes are not involved in the infection process, as seems to be the case for
255 MoMyb8 (Lee et al., 2021). Nevertheless, since all genes are expressed well in planta at different
256 stages of plant infection (**Table S2**), we suggest that the explanation is redundancy in function or
257 genetic compensation for most of these gene deletions often found negating phenotypic effects of
258 knockouts (El-Brolosy and Stainier, 2017). Similar regulated genes not belonging to the Myb-
259 containing genes or regulated by the Myb genes can create this redundancy or genetic
260 compensation (**Fig. 8, S5,** and **Table S2**). Such genes might collaborate with the deleted genes at
261 different time points or by upregulation of genes with similarity in amino acid sequence with
262 overlapping functions since we found the MoMyb-genes sort into 4 clusters of similarity (**Fig. 1B**).
263 Of course, the 5 genes we could not delete that have not been deleted before (*momyb11, 12, 14,*
264 *17, and 19*) could have a role in pathogenicity. If these are genuinely essential for growth in culture,
265 and because of that cannot be deleted, they naturally have a profound effect on pathogenicity

since they might be essential for survival also during infection. Interestingly these potentially essential genes are members of different co-regulated clusters identified (**Fig. 8 and S5**), making it possible for them to encode proteins that act together with the other Myb proteins and take over their functions.

A gene encoding a Myb protein that affected both growth and infection phenotypes is *MoMyb13*. This protein is large (**Fig. 1A**) and has no orthologues outside Ascomycota in the NCBI database. We investigated it further through bioinformatics and found similar large proteins predicted in 19 other published genomes (**Fig. S6**). Three of these hits were in other strains of *Pyricularia oryzae* (*M. oryzae* teleomorph), which is not strange. Maybe more interesting, common to all hits, including the ones in *M.oryzae*, they are all fungi known to produce melanized hydrophobic structures (Collado et al., 2002; Liu et al., 2009; Kokaew et al., 2011; Al-Khawaldeh et al., 2020; Geisen et al., 2021; Sarsaiya et al., 2020; Li et al., 2016; Gao et al., 2021; Chen et al., 2021) suggesting that a possible involvement of MoMyb13 in hydrophobins formed together with melanin production could be relevant also for these similar proteins in diverse fungi all belonging to the class Sordariomycetes.

Interestingly, all these melanized fungi are known to grow endophytically, as *M. oryzae* do in the first biotrophic stages of infection (Kankanala et al., 2007) when *MoMyb13* is specifically upregulated (**Fig. 8 and Fig. S5).** If these genes and gene products have similar functions as in *M. oryzae* is unknown. Future research should investigate whether these genes from the other fungi could complement *MoMyb13* or each other since *MoMyb13* seems essential in the early biotrophic establishment stage of *M. oryzae* infection of rice. The orthologues of its gene's products are only present in relatively closely related ascomycetes having biotrophic/endophytic relationships with plants (**Fig. S6**), suggesting that this gene and its product have some essential function for establishing biotrophic interactions. The *MoMyb13* gene or its gene product could also potentially be targeted by more pathogen-specific control measures since it does not seem widely spread among fungi outside the class Sordariomycetes.

The other gene that showed changed strain phenotypes when deleted was *MoMyb15*, which encodes for an ISW2-like protein containing a SANT-type Myb domain. MoMyb15 is at NCBI annotated as an ISW2 type Myb-containing protein conserved in eukaryotes. A true MoISW2 is potentially involved in gene regulation by regulating the access of transcription factors by binding to DNA and controlling nucleosome positioning regulating the access of DNA for other transcription factors and repressors instead of being a transcription factor itself (Fazzio et al., 2005; Hada et al., 2019; Kagalwala et al., 2004). It would be interesting to confirm this function and focus on which DNA sequences it binds to (CHP-seq) and the regulatory effect of the deletion on genes physically adjacent to the DNA binding site in the genome. According to our results (**Fig. 8 and S5 and Table S2**), the *MoMyb15* gene is upregulated at HPIs at the transition from biotrophy to necrotrophy (Kankanala et al., 2007), suggesting it could be a "master regulator" for regulating the fungus many defenses against plant defenses that are strongly upregulated in the biotrophy/necrotrophy transition and during the necrotrophic stage (Kou et al., 2019). Thus, we have initiated detailed research on MoMyb15 to investigate if it has a "master regulator" function working through nucleosome condensation in *M. oryzae*.

The genes encoding proteins with Myb-domains showing no phenotypes when deleted should also be subject to studies since they were upregulated at specific infection stages. However, these genes could be studied using knockdown systems to avoid mutation-induced genetic compensation (El-Brolosy and Stainier, 2017). Conditional knockdown systems can maybe be used for essential genes we did not manage to knock out, even if the most common TET-on TET-off can create artifacts due to mitochondrial poisoning (Moullan et al., 2015).

METHODS

Organisms and media used

Magnaporthe oryzae B. Couch anamorph of the teleomorph *Pyricularia oryzae* Cavara was used for this research. As background *M. oryzae* strain, we used Ku80 to minimize random integration events when transformed (Villalba et al., 2008). The susceptible Indica rice (cv. CO-39) and barley (cv. Golden Promise) used for the fungal pathogenicity tests were from the seed bank of our laboratory. The CM (complete medium), MM (minimal medium), and RBM (rice bran medium) used for growing the fungus were prepared as described (Li et al., 2019). The *Escherichia coli* strain DH-5α used for routine bacterial transformations (Li et al., 2015) and maintenance of various plasmid vectors was bought from Solarbio Life Sciences, China.

Knockouts, complementations, and verifications

The *Myb* gene deletion vectors were constructed by inserting the 1 kb up-and-down-stream fragments of the target gene's coding region as the flanking regions of the HPH (hygromycin phosphotransferase) gene of the plasmid pBS-HYG (Li et al., 2012). No less than 2 μg of the deletion vector DNA of the target gene was introduced to Ku80 protoplasts, and transformants were selected for hygromycin resistance to perform gene deletion transformations. Southern blotting was conducted to confirm the correct deletion using the digoxigenin (DIG) high prime DNA labeling and detection starter Kit I (11745832910 Roche Germany). The *Myb* gene complementation vectors were constructed by cloning the entire length of the target gene with the native promoter region (about 1.5-kb) to the pCB1532 plasmid. When making the complementation vector, *GFP* was linked to the C-terminal of the target genes to study the sub-cellar localization of Myb proteins. The constructed vector DNA was introduced into the mutation protoplast for the gene complementation assay, and the transformants were screened using 50 μg/ml chlorimuron-ethyl to select successful complementation strains. The detailed fungal protoplast preparation and transformation methods have been described previously (Li et al., 2016). All primers needed for these knockouts and complementations are listed (**Table S1**). The sub-cellar localization of Myb proteins was observed by confocal microscopy (Nikon A1). GFP and RFP excitation wavelengths were 488 nm and 561 nm, respectively.

Colony and growth phenotypes measurements

Vegetative growth was tested by measuring the colony diameter after ten days of growth in 9 cm Petri dishes at 25℃ under 12h-to-12h light and dark periods. Conidia production was evaluated by flooding the 12-day-old colony with double distilled water, filtering out the mycelia with gauze, and counting the conidia using a hemacytometer. The conidiophore induction assay was performed by

353 excising one thin agar block from the fungal colony and then incubating it in a sealed chamber for
354 24 h with constant light (Li et al., 2010b). Mycelia appressoria were induced by placing a suspension
355 of mycelial fragments on a hydrophobic surface in a humid environment at 25℃ for 24h. The
356 pathogenicity assay on rice was performed by spraying 5 ml conidial suspension (5×104 spores/ml)
357 on 15-day-old plants (Li et al., 2014). Post-spraying inoculated plants were kept in a sealed chamber
358 with a 90% relative humidity at 25℃ for 24 h. Then, the inoculated plants were removed from the
359 chamber to allow disease symptoms to develop for 4-5 days. The pathogenicity assay on excised
360 barley and rice leaves was performed by cutting a small block from the agar culture of the fungus
361 and placing it on excised leaves for five days in a moist chamber for disease development (Li et al.,
362 2010a). The sexual reproduction was performed by crossing the tested strain with the sexually
363 compatible strain TH3 in OM plates and then incubating at 19℃ for 30 days with continuous light.
364 The perithecia and clavate asci were photographed by a microscope equipped with a camera
365 (OLYMPUS BX51).
366
367 **RT-qPCR**
368
369 Total RNA was extracted using Eastep®Super Total RNA Extraction Kit (Promega (Beijing)
370 Biotechnology, LS1040) to perform RT-qPCR, and 5 mg of RNA was reverse-transcribed to cDNA
371 using the Evo M-MLV RT kit with gDNA to clean before the qPCR (Accurate Biotechnology (Hunan),
372 AG11705) according to the manufacturer's instructions. The resulting cDNA was diluted ten times
373 and used as the template for qPCR. The qPCR reactions were performed using an Applied
374 Biosystems 7500 Real-Time PCR System. Each reaction contained 25 ul of SuperRealPreMix Plus
375 SYBR Green (Tiangen Biotechnology, Beijing, FP205-02), one μl of cDNA, and 1.5 μl of each primer
376 solution. The thermal cycling conditions were 15 min at 95 ℃ followed by 40 cycles of 10 s at 95 ℃
377 and 20 s at 60 ℃. The threshold cycle (Ct) values were obtained by analyzing amplification curves
378 with a normalized reporter threshold of 0.1. The relative expression value was calculated using the
379 $2^{-\Delta\Delta CT}$ method (Livak and Schmittgen, 2001).
380
381 **PCA analysis and clustering of RT-qPCR expression data**
382
383 First, expression values were normalized using the beta-tubulin gene as the housekeeping
384 reference gene. Since we did not want to give too much weight to the very artificial conditions in
385 lab media for mycelium growth (MY), average expression at all the measured HPIs was used for
386 normalization to focus on the *in planta* variation at different HPIs and to make comparisons of gene
387 expression profiles during infection of rice more critical for the analysis. For the PCA, we used
388 correlation of the data for the different genes since the genes have different averages of expression.
389 Together that focuses the analysis on the genes' varying HPI profiles and makes them comparable.
390 The analysis is shown as a PCA bi-plot, of the PC1 and PC2 with gene names as objects, the variables
391 vectorial contributions to the PCs (the different time HPIs, MY=mycelium in culture, and Con =
392 conidia before inoculation) (**Fig. S5).** We used the freeware PAST (Hammer et al., 2001) version
393 4.08 (released November 2021) for the PCA analysis. It is available from the University of Oslo,
394 Natural History Museum https://www.nhm.uio.no/english/research/infrastructure/past/. The
395 data was entered and handled in MS Excel and then copy-pasted into PAST for analysis. The same
396 data is, in addition, presented using the clustering function in PAST to present the data in a more

usual way using a clustering method that gives a similar result as the Minimum spanning tree (Neighbor-joining, Gower similarity, Final branch as root) (**Fig. 8**) and presented with the same color coding as in **Figure 1b** for comparison.

Author contributions:

YL, domain prediction and evolutionary analysis, Myb gene deletions, phenotype tests, protein localization, RT-qPCR, data collection and analysis, figure making, manuscript preparation, and writing. XZ, MoMyb13 gene deletion, MoMyb13 mutant phenotype analysis, MoMyb13 protein localization, RT-qPCR of hydrophobin gene. MC, MP, CL, LG, PH, Myb-gene deletions. SZ, RT-qPCR of all Myb genes, protein localization of 8 Myb genes. SO, RT-qPCR extended analysis including PCA and clustering, extended analysis of possible roles of Myb13 and Myb15, manuscript preparation, and writing.

Acknowledgments

The strain Ku80 used in this study was obtained initially from Nicholas J. Talbot, University of Exeter, UK. This research was financially supported by the National Science Foundation of China (NSFC31871914)

CONFLICT OF INTEREST

The authors declare that the research was conducted without any commercial or financial relationships that could be construed as a potential conflict of interest.

DATA AVAILABILITY STATEMENT

Data supporting the findings of this study are available within the paper and its supplements.

423 **Figure Legends**
424
425 **Figure 1**. Domain structure of the identified genes encoding for Myb domain-containing proteins
426 and their sequence similarities. (**A**) Identified conserved domains in the found Myb domain-
427 containing proteins. (**B**) The similarity analysis of predicted amino acid sequences showed that the
428 19 proteins could be sorted into 4 groups marked by the color code.
429
430 **Figure 2**. The radial growth rate of *Δmomyb2, Δmomyb13*, and *Δmomyb15* are slower than in the
431 background strain Ku80. (**A**) Images of the morphology of the different strains on the three
432 different media, complete medium (CM), minimal medium (MM), and rice bran medium (RBM). (**B**)
433 Measured colony diameter after 10day incubation in alternating dark/light (12h/12h) at 25 ^{O}C. (**C**)
434 Growth inhibition in deletion strains was measured as colony diameter after 10-day incubation in
435 alternating dark/light (12h/12h) at 25 ^{O}C compared to the background strain Ku80. Bars indicate
436 SEM and bars with the same letters are not significantly different (P>0.05; t-test).
437
438 **Figure 3.** MoMyb13 and MoMyb15 are involved in *M. oryzae* pathogenicity since mutants of the
439 genes showed reduced lesions when tested with the agar block technique on excised barley and
440 rice leaves, but this lack of lesion is not the result of lack of mycelia appressorium formation. Test
441 of mutants and background strain on intact (**A**) and wounded (**B**) barley leaves. Test of mutants and
442 background strain on intact (**C**) and wounded (**D**) rice leaves. Mycelia appressorium formation from
443 mycelial fragments on a hydrophobic surface (**E**).
444
445 **Figure 4.** *Δmomyb13* and *Δmomyb15* make no conidia, while Ku80 and complement strains readily
446 make. (**A**) Conidiophore morphology and conidiation. (**B**) Conidia production on CM and RBM.
447
448 **Figure 5.** Hydrophobin production, necessary for producing hydrophobic arial conidia-producing
449 mycelium, by MPG1 is downregulated in *Δmomyb13,* but overexpression of the MPG1 gene in the
450 *Δmomyb13* strain does not restore pathogenicity. (**A**) colonies of *Δmomyb13* are easily wettable,
451 while the surface of the background strain (Ku80), the complementation strain, or the *Δmomyb13*
452 strain containing the overexpressed hydrophobin *MPG1* (*Δmomyb13-11/TrpC-MPG1*) is not
453 wettable. (**B**) Percent change in expression of 4 hydrophobin genes in *Δmomyb13* h compared to
454 *Ku80*, showing that *MPG1* is severely downregulated while the others are less affected. (**C**) Percent
455 change in *MPG1* expression in *Ku80*, *Δmomyb13 and Δmomyb13/TrpC-MPG1* strains compared to
456 *Ku80*. (**D**) Leaf lesions formed by the *Ku80*, *Δmomyb13,* and *Δmomyb13/TrpC-MPG1* strains using
457 the agar block technique. Error bars in (A) and (C) show the 95% confidence intervals. Bars with
458 confidence intervals not overlapping with other bars' confidence intervals or levels (as zero) are
459 significantly different (P<0.05 for the null hypothesis that they are the same).
460
461 **Figure 6**. The three mutants, *Δmomyb5, Δmomyb13*, and *Δmomyb15,* showed reduced stress
462 tolerance compared to the background strain Ku80 using a standard panel of stress treatments. (**A**)
463 Colony size and morphology of Ku80, the mutants, and the complements after 10 days in
464 alternating dark/light (12h/12h) at 25°C growing on CM or CM with additions of SDS, CR, NaCl SOR,
465 or H_2O_2 as stresses (see methods). (**B**) Same as in (**A**) but shows the average of 3 replicates with

466 error bars. Error bars show the standard error means of the respective averages, and stars mark
467 statistical differences compared to Ku80.
468
469 **Figure 7.** All three *momyb*-deletions that showed phenotypes differing from Ku80 (*Δmomyb13*,
470 *Δmomyb2,* and *Δmomyb15*) localize to conidia, appressorial, and mycelial nuclei as indicated by co-
471 localization with the mCherry labeled nuclear marker MoHis1-mCherry confirming that they are
472 indeed localized to nuclei as expected. (**A**) MoMyb13-GFP localizes to nuclei. (**B**) MoMyb2-GFP
473 localizes to nuclei but mainly to what is most probably the nucleoli. (**C**) MoMyb15-GFP localizes to
474 nuclei. DIC= Differential Interference Contrast.
475
476 **Figure 8.** The different *MoMyb* genes show different expression profiles. The expression profiles
477 cluster into 5 groups depending on hours post-infection (HPI) expression during infection. This
478 clustering is, in principle, similar to what can be seen in the PCA plot (**Fig. S5**). Transcripts from
479 growth on agar medium (MY), conidia (late in the formation of conidia), and in rice plant leaves at
480 8 HPI (8h), 24 HPI (24h), 48 HPI (48h), 72 HPI (72h), and 96 HPI (96h). The color code used is the
481 same as in **Fig. 1B** for the phylogeny clusters showing that the regulatory sub-clusters activated at
482 different HPI contain sets of genes with little similarity in sequence homology. Ellipses mark the 3
483 genes with phenotypes different from Ku80 for their respective deletion mutants.
484
485 **Table 1.** Phenotype summary of MoMybs.
486
487 **Figure S1.** Southern blot confirmation for all the 12 mutants obtained in this study. The HPH gene
488 or the 1.0 kb up- or downstream of the target gene was used as a probe to detect successful gene
489 knockout events.
490
491 **Figure S2.** Colony morphology of the 9 *Myb* gene mutants with no effect on pathogenicity
492 compared to Ku80 on CM (A) MM (B), and RBM (C).
493
494 **Figure S3**. No effect on pathogenicity due to the *Myb* gene mutations can be seen for 9 mutants
495 tested using either the agar block technique or conidia sprayed on the leaves. (**A**) Test of mutants
496 and background strain (Ku80) on barley leaves using the agar block technique (**B**) Test of mutants
497 and background strain (Ku80) conidia sprayed on rice leaves.
498
499 **Figure S4**. Localization of the MoMyb-GFP complements from which we could find strong enough
500 GFP signals in mycelia conidia and appressoria. The localization pattern suggests nuclear
501 localisations as expected for Myb-domain-containing proteins.
502
503 **Figure S5.** The *MoMyb* genes show different expression profiles visualized by Principal Component
504 Analysis (PCA). Variables were transcription with different treatments and HPIs from infected rice
505 leaves, growth on agar medium (MY), conidia (Conidia late), 8 HPI (8h), 24 HPI (24h), 48 HPI (48h),
506 72 HPI (72h) and 96 HPI (96h). The expression values of the 19 identified genes encoding Myb
507 domain-containing proteins were the objects. The first and second PCA are presented after a PCA
508 based on the correlation of the expression profiles (as shown in **Table S2**). The plot is a biplot also
509 showing the loading of the variables in the two PCs. A "Minimum spanning tree" nearly identical

510 to the tree in Fig. 8 joins the most similar expressed genes for all calculated PCs. The color code
511 used for the marker dots (or Xs) in front of the gene names is the same as in **Fig. 1B** for the
512 predicted amino acid sequence similarity clusters, showing that the regulatory clusters contain sets
513 of genes with little similarity in sequence homology. A marker X in front of the gene name shows a
514 gene we could not delete. Boxes mark the 3 genes with noted phenotypes for their deletion
515 mutants. MoMyb1, furthest to the left in the figure, is known from the literature to be activated
516 early in infection, and here it is far left in component 1 with the 8 HPI negative loading
517 corroborating the previous results from the literature.
518
519 **Figure S6.** Alignments of the most similar orthologues to the MoMyb13 protein from species
520 related to *M. oryzae* (*Pyricularia oryzae*)(all are with E-values less or equal to 3E-135 and with more
521 than 70% query cover) (**Table S3**). Data from an NCBI produced by the alignment of all fungal
522 genomes annotated.
523
524 **Table S1.** Primers used in this study, their sequences, and what they were used to accomplish.
525
526 **Table S2.** List of the MoMyb proteins organized in groups after their judged expression profiles.
527 Deleted genes in this study are marked by an X in or a 0 if not deleted. The relative expression in
528 normalized by the average expression during infection (HPI8-96) for each gene (the HPI columns)
529 shown in columns. MY=in vitro mycelium), Con= conidia, then 8-96HPI columns. Profile shows the
530 profile My-Con-8hpi-24hpi-48hpi-72hpi-96hpi. The transition from biotrophy to necrotrophy
531 occurs at around 48hpi or just before. Infection and entry into biotrophy are during the first 24
532 hours. The two first, MY and Con shows expression in vitro and conidia before penetration of the
533 leaf. Comments to the far right tell when the respective groups of genes are relatively highly
534 expressed compared to their respective averages during infection.
535
536 **Table S3.** The similarity of NCBI hit data of all highly similar orthologues to MoMyb13 (E value less
537 or equal 3E-135), other strains of M. oryzae (Pyricularia oryzae) excluded. With more than 70%
538 query cover.
539

References

Al-Khawaldeh, M.M., Araj, S.-E., Alananbeh, K.M. & Antary, T.M.A. (2020) Wheat Cultivable Fungal Endophytes in Jordan. *Fresenius Environmental Bulletin*, 29, 13.

Allan, A.C. & Espley, R.V. (2018) MYBs Drive Novel Consumer Traits in Fruits and Vegetables. *Trends in Plant Science*, 23, 693–705. https://doi.org/10.1016/j.tplants.2018.06.001.

Baldoni, E., Genga, A. & Cominelli, E. (2015) Plant MYB Transcription Factors: Their Role in Drought Response Mechanisms. *Int. J. Mol. Sci.*, 41.

Bayry, J., Aimanianda, V., Guijarro, J.I., Sunde, M. & Latgé, J.-P. (2012) Hydrophobins—Unique Fungal Proteins Heitman, J. (Ed.). *PLoS Pathogens*, 8, e1002700. https://doi.org/10.1371/journal.ppat.1002700.

Beckerman, J.L. (1996) MPG1, a Gene Encoding a Fungal Hydrophobin of *Magnaporthe grisea*, Is Involved in Surface Recognition. *Molecular Plant-Microbe Interactions*, 9, 450. https://doi.org/10.1094/MPMI-9-0450.

Berger, B.W. & Sallada, N.D. (2019) Hydrophobins: Multifunctional Biosurfactants for Interface Engineering. *Journal of Biological Engineering*, 13, 10. https://doi.org/10.1186/s13036-018-0136-1.

Cao, Y., Chen, J., Xie, X., Liu, S., Jiang, Y., Pei, M., et al. (2022) Characterization of two infection-induced transcription factors of *Magnaporthe oryzae* reveals their roles in regulating early infection and effector expression. *Molecular Plant Pathology*, 23, 1200–1213. https://doi.org/10.1111/mpp.13224.

Cao, Y., Li, K., Li, Y., Zhao, X. & Wang, L. (2020) MYB Transcription Factors as Regulators of Secondary Metabolism in Plants. *Biology*, 9, 61. https://doi.org/10.3390/biology9030061.

Chen, H., Mao, L., Zhao, N., Xia, C., Liu, J., Kubicek, C.P., et al. (2021) Verification of TRI3 Acetylation of Trichodermol to Trichodermin in the Plant Endophyte *Trichoderma taxi*. *Frontiers in Microbiology*, 12, 731425. https://doi.org/10.3389/fmicb.2021.731425.

Collado, J., Gonzalez, A., Platas, G., Stchigel, A.M., Guarro, J. & Pelaez, F. (2002) *Monosporascus ibericus* sp. nov., an Endophytic Ascomycete from Plants on Saline Soils, with Observations on the Position of the Genus based on Sequence Analysis of the 18S rDNA. *Mycological Research*, 106, 118–127. https://doi.org/10.1017/S0953756201005172.

Dean, R.A., Talbot, N.J., Ebbole, D.J., Farman, M.L., Mitchell, T.K., Orbach, M.J., et al. (2005) The Genome Sequence of the Rice Blast Fungus *Magnaporthe grisea*. *Nature*, 434, 980–986. https://doi.org/10.1038/nature03449.

Dong, Y., Zhao, Q., Liu, X., Zhang, X., Qi, Z., Zhang, H., et al. (2015) MoMyb1 is Required for Asexual Development and Tissue-specific Infection in the Rice Blast Fungus *Magnaporthe oryzae*. *BMC Microbiology*, 15, 37. https://doi.org/10.1186/s12866-015-0375-y.

Du, H., Zhang, L., Liu, L., Tang, X.-F., Yang, W.-J., Wu, Y.-M., et al. (2009) Biochemical and Molecular Characterization of Plant MYB Transcription Factor Family. *Biochemistry (Moscow)*, 74, 1–11. https://doi.org/10.1134/S0006297909010015.

Dubos, C., Stracke, R., Grotewold, E., Weisshaar, B., Martin, C. & Lepiniec, L. (2010) MYB Transcription Factors in *Arabidopsis*. *Trends in Plant Science*, 15, 573–581. https://doi.org/10.1016/j.tplants.2010.06.005.

Ebbole, D.J. (2007) Magnaporthe as a Model for Understanding Host-Pathogen Interactions. *Annual Review of Phytopathology*, 45, 437–456. https://doi.org/10.1146/annurev.phyto.45.062806.094346.

El-Brolosy, M.A. & Stainier, D.Y.R. (2017) Genetic Compensation: A Phenomenon in Search of Mechanisms Moens, C. (Ed.). *PLOS Genetics*, 13, e1006780. https://doi.org/10.1371/journal.pgen.1006780.

Eme, L., Spang, A., Lombard, J., Stairs, C.W. & Ettema, T.J.G. (2017) Archaea and the Origin of Eukaryotes. *Nature Reviews Microbiology*, 15, 711–723. https://doi.org/10.1038/nrmicro.2017.133.

Fazzio, T.G., Gelbart, M.E. & Tsukiyama, T. (2005) Two Distinct Mechanisms of Chromatin Interaction by the Isw2 Chromatin Remodeling Complex in vivo. *Molecular and Cellular Biology*, 25, 9165–9174. https://doi.org/10.1128/MCB.25.21.9165-9174.2005.

Gao, H., Pan, M., Tian, C. & Fan, X. (2021) *Cytospora* and *Diaporthe* Species Associated With Hazelnut Canker and Dieback in Beijing, China. *Frontiers in Cellular and Infection Microbiology*, 11, 664366. https://doi.org/10.3389/fcimb.2021.664366.

Geisen, S., Hooven, F.C., Kostenko, O., Snoek, L.B. & Putten, W.H. (2021) Fungal Root Endophytes Influence Plants in a Species-specific Manner that depends on Plant's Growth Stage Vries, F. (Ed.). *Journal of Ecology*, 109, 1618–1632. https://doi.org/10.1111/1365-2745.13584.

Gladieux, P., Condon, B., Ravel, S., Soanes, D., Maciel, J.L.N., Nhani, A., et al. (2018) Gene Flow between Divergent Cereal- and Grass-Specific Lineages of the Rice Blast Fungus *Magnaporthe oryzae* Taylor, J.W. (Ed.). *mBio*, 9. https://doi.org/10.1128/mBio.01219-17.

Gostinčar, C., Lenassi, M., Gunde-Cimerman, N. & Plemenitaš, A. (2011) Fungal

Adaptation to Extremely High Salt Concentrations. Advances in Applied Microbiology. Elsevier, pp. 71–96.

Hada, A., Hota, S.K., Luo, J., Lin, Y., Kale, S., Shaytan, A.K., et al. (2019) Histone Octamer Structure Is Altered Early in ISW2 ATP-Dependent Nucleosome Remodeling. *Cell Reports*, 28, 282-294.e6. https://doi.org/10.1016/j.celrep.2019.05.106.

Hogues, H., Lavoie, H., Sellam, A., Mangos, M., Roemer, T., Purisima, E., et al. (2008) Transcription Factor Substitution during the Evolution of Fungal Ribosome Regulation. *Molecular Cell*, 29, 552–562. https://doi.org/10.1016/j.molcel.2008.02.006.

Howard, R.J., Ferrari, M.A., Roach, D.H. & Money, N.P. (1991) Penetration of hard Substrates by a Fungus employing Enormous Turgor Pressures. *Proceedings of the National Academy of Sciences*, 88, 11281–11284. https://doi.org/10.1073/pnas.88.24.11281.

Islam, M.T., Croll, D., Gladieux, P., Soanes, D.M., Persoons, A., Bhattacharjee, P., et al. (2016) Emergence of Wheat Blast in Bangladesh was caused by a South American Lineage of *Magnaporthe oryzae*. *BMC Biology*, 14, 84. https://doi.org/10.1186/s12915-016-0309-7.

Kagalwala, M.N., Glaus, B.J., Dang, W., Zofall, M. & Bartholomew, B. (2004) Topography of the ISW2–nucleosome Complex: Insights into Nucleosome Spacing and Chromatin Remodeling. *The EMBO Journal*, 23, 2092–2104. https://doi.org/10.1038/sj.emboj.7600220.

Kankanala, P., Czymmek, K. & Valent, B. (2007) Roles for Rice Membrane Dynamics and Plasmodesmata during Biotrophic Invasion by the Blast Fungus. *The Plant Cell*, 19, 706–724. https://doi.org/10.1105/tpc.106.046300.

Kim, Y., Kim, H., Son, H., Choi, G.J., Kim, J.-C. & Lee, Y.-W. (2014) MYT3, A Myb-Like Transcription Factor, Affects Fungal Development and Pathogenicity of Fusarium graminearum Yu, J.-H. (Ed.). *PLoS ONE*, 9, e94359. https://doi.org/10.1371/journal.pone.0094359.

Kokaew, J., Manoch, L., Worapong, J., Chamswarng, C., Singburaudom, N., Visarathanonth, N., et al. (2011) *Coniochaeta ligniaria* an Endophytic Fungus from *Baeckea frutescens* and Its Antagonistic Effects Against Plant Pathogenic Fungi. 44, 9.

Kou, Y., Qiu, J. & Tao, Z. (2019) Every Coin Has Two Sides: Reactive Oxygen Species during Rice–*Magnaporthe oryzae* Interaction. *International Journal of Molecular Sciences*, 20, 1191. https://doi.org/10.3390/ijms20051191.

Lee, S., Völz, R., Song, H., Harris, W. & Lee, Y.-H. (2021) Characterization of the

MYB Genes Reveals Insights Into Their Evolutionary Conservation, Structural Diversity, and Functional Roles in Magnaporthe oryzae. *Frontiers in Microbiology*, 12, 721530. https://doi.org/10.3389/fmicb.2021.721530.

Li, H., Lu, J., Liu, X., Xhang, L. & Lin, F. (2012) Vector Building and Usage for Gene Knockout, Protein Expression and Fluorescent Fusion Protein in The Rice Blast Fungus. *Journal of Agricultural Biotechnology*, 20, 94–104. https://doi.org/10.3969/j.issn.1674-7968.2012.01.013.

Li, J., Han, G., Sun, C. & Sui, N. (2019) Research Advances of MYB Transcription Factors in Plant Stress Resistance and Breeding. *Plant Signaling & Behavior*, 14, 1613131. https://doi.org/10.1080/15592324.2019.1613131.

Li, T., Wang, X., Luo, J., Yang, M. & Kong, L. (2016) Antioxidant Sordariol Dimers from *Sordaria macrospora* and the absolute Configuration Determinations of their two Simultaneous Linear 1,2-diols. *Tetrahedron Letters*, 57, 2754–2757. https://doi.org/10.1016/j.tetlet.2016.05.014.

Li, Y., Liang, S., Yan, X., Wang, H., Li, D., Soanes, D.M., et al. (2010a) Characterization of *MoLDB1* Required for Vegetative Growth, Infection-Related Morphogenesis, and Pathogenicity in the Rice Blast Fungus *Magnaporthe oryzae*. *Molecular Plant-Microbe Interactions®*, 23, 1260–1274. https://doi.org/10.1094/MPMI-03-10-0052.

Li, Y., Que, Y., Liu, Y., Yue, X., Meng, X., Zhang, Z., et al. (2015) The Putative Gγ Subunit Gene MGG1 is required for Conidiation, Appressorium Formation, mating and Pathogenicity in *Magnaporthe oryzae*. *Current Genetics*, 61, 641–651. https://doi.org/10.1007/s00294-015-0490-1.

Li, Y., Yan, X., Wang, H., Liang, S., Ma, W.-B., Fang, M.-Y., et al. (2010b) MoRic8 Is a Novel Component of G-Protein Signaling During Plant Infection by the Rice Blast Fungus *Magnaporthe oryzae*. *Molecular Plant-Microbe Interactions®*, 23, 317–331. https://doi.org/10.1094/MPMI-23-3-0317.

Li, Y., Yue, X., Que, Y., Yan, X., Ma, Z., Talbot, N.J., et al. (2014) Characterisation of Four LIM Protein-Encoding Genes Involved in Infection-Related Development and Pathogenicity by the Rice Blast Fungus *Magnaporthe oryzae* Xue, C. (Ed.). *PLoS ONE*, 9, e88246. https://doi.org/10.1371/journal.pone.0088246.

Lin, Y., Son, H., Lee, J., Min, K., Choi, G.J., Kim, J.-C., et al. (2011) A Putative Transcription Factor MYT1 Is Required for Female Fertility in the Ascomycete Gibberella zeae Yu, J.-H. (Ed.). *PLoS ONE*, 6, e25586. https://doi.org/10.1371/journal.pone.0025586.

Lin, Y., Son, H., Min, K., Lee, J., Choi, G.J., Kim, J.-C., et al. (2012) A Putative Transcription Factor MYT2 Regulates Perithecium Size in the Ascomycete

Gibberella zeae Yu, J.-H. (Ed.). *PLoS ONE*, 7, e37859. https://doi.org/10.1371/journal.pone.0037859.

Liu, J., Osbourn, A. & Ma, P. (2015) MYB Transcription Factors as Regulators of Phenylpropanoid Metabolism in Plants. *Molecular Plant*, 8, 689–708. https://doi.org/10.1016/j.molp.2015.03.012.

Liu, K., Ding, X., Deng, B. & Chen, W. (2009) Isolation and Characterization of Endophytic Taxol-producing Fungi from *Taxus chinensis*. *Journal of Industrial Microbiology & Biotechnology*, 36, 1171–1177. https://doi.org/10.1007/s10295-009-0598-8.

Livak, K.J. & Schmittgen, T.D. (2001) Analysis of Relative Gene Expression Data Using Real-Time Quantitative PCR and the 2−ΔΔCT Method. *Methods*, 25, 402–408. https://doi.org/10.1006/meth.2001.1262.

Ma, D. & Constabel, C.P. (2019) MYB Repressors as Regulators of Phenylpropanoid Metabolism in Plants. *Trends in Plant Science*, 24, 275–289. https://doi.org/10.1016/j.tplants.2018.12.003.

Malaker, P.K., Barma, N.C.D., Tiwari, T.P., Collis, W.J., Duveiller, E., Singh, P.K., et al. (2016) First Report of Wheat Blast Caused by *Magnaporthe oryzae* Pathotype *triticum* in Bangladesh. *Plant Disease*, 100, 2330–2330. https://doi.org/10.1094/PDIS-05-16-0666-PDN.

Mateos, L., Jiménez, A., Revuelta, J.L. & Santos, M.A. (2006) Purine Biosynthesis, Riboflavin Production, and Trophic-Phase Span Are Controlled by a Myb-Related Transcription Factor in the Fungus *Ashbya gossypii*. *Applied and Environmental Microbiology*, 72, 5052–5060. https://doi.org/10.1128/AEM.00424-06.

Matheis, S., Yemelin, A., Scheps, D., Andresen, K., Jacob, S., Thines, E., et al. (2017) Functions of the Magnaporthe oryzae Flb3p and Flb4p transcription factors in the regulation of conidiation. *Microbiological Research*, 196, 106–117. https://doi.org/10.1016/j.micres.2016.12.010.

Mitra, P. (2018) Transcription Regulation of MYB: a Potential and Novel Therapeutic Target in Cancer. *Annals of Translational Medicine*, 6, 443–443. https://doi.org/10.21037/atm.2018.09.62.

Moullan, N., Mouchiroud, L., Wang, X., Ryu, D., Williams, E.G., Mottis, A., et al. (2015) Tetracyclines Disturb Mitochondrial Function across Eukaryotic Models: A Call for Caution in Biomedical Research. *Cell Reports*, 10, 1681–1691. https://doi.org/10.1016/j.celrep.2015.02.034.

Mukherjee, K., Pandey, D.M. & Vidyarthi, A.S. (2012) Molecular Dynamics Simulation of Rap1 Myb-type domain in Saccharomyces cerevisiae.

Bioinformation, 8, 881–885. https://doi.org/10.6026/97320630008881.

Pattabiraman, D.R. & Gonda, T.J. (2013) Role and Potential for Therapeutic targeting of MYB in Leukemia. *Leukemia*, 27, 269–277. https://doi.org/10.1038/leu.2012.225.

Pennisi, E. (2010) Armed and Dangerous. *Science*, 327, 804–805. https://doi.org/10.1126/science.327.5967.804.

Prouse, M.B. & Campbell, M.M. (2012) The Interaction Between MYB Proteins and their Target DNA binding Sites. *Biochimica et Biophysica Acta (BBA) - Gene Regulatory Mechanisms*, 1819, 67–77. https://doi.org/10.1016/j.bbagrm.2011.10.010.

Ramos-Sáenz, A., González-Álvarez, D., Rodríguez-Galán, O., Rodríguez-Gil, A., Gaspar, S.G., Villalobo, E., et al. (2019) Pol5 is an essential ribosome biogenesis factor required for 60S ribosomal subunit maturation in *Saccharomyces cerevisiae*. *RNA*, 25, 1561–1575. https://doi.org/10.1261/rna.072116.119.

Rodríguez-Sánchez, L., Rodríguez-López, M., García, Z., Tenorio-Gómez, M., Schvartzman, J.B., Krimer, D.B., et al. (2011) The fission yeast rDNA-binding protein Reb1 regulates G1 phase under nutritional stress. *Journal of Cell Science*, 124, 25–34. https://doi.org/10.1242/jcs.070987.

Roy, S. (2016) Function of MYB Domain Transcription Factors in Abiotic Stress and Epigenetic Control of Stress Response in Plant Genome. *Plant Signaling & Behavior*, 11, e1117723. https://doi.org/10.1080/15592324.2015.1117723.

Sakulkoo, W., Osés-Ruiz, M., Oliveira Garcia, E., Soanes, D.M., Littlejohn, G.R., Hacker, C., et al. (2018) A Single Fungal MAP Kinase controls Plant Cell-to-cell invasion by The Rice Blast Fungus. *Science*, 359, 1399–1403. https://doi.org/10.1126/science.aaq0892.

Sarsaiya, S., Jain, A., Fan, X., Jia, Q., Xu, Q., Shu, F., et al. (2020) New Insights into Detection of a Dendrobine Compound From a Novel Endophytic Trichoderma longibrachiatum Strain and Its Toxicity Against Phytopathogenic Bacteria. *Frontiers in Microbiology*, 11, 337. https://doi.org/10.3389/fmicb.2020.00337.

Valsecchi, I., Sarikaya-Bayram, Ö., Wong Sak Hoi, J., Muszkieta, L., Gibbons, J., Prevost, M.-C., et al. (2017) MybA, a transcription factor involved in conidiation and conidial viability of the human pathogen *Aspergillus fumigatus*: A transcription factor regulating conidiation in *Aspergillus*. *Molecular Microbiology*, 105, 880–900. https://doi.org/10.1111/mmi.13744.

Verma, S., Gazara, R.K. & Verma, P.K. (2017) Transcription Factor Repertoire of Necrotrophic Fungal Phytopathogen *Ascochyta rabiei*: Predominance of MYB Transcription Factors As Potential Regulators of Secretome. *Frontiers in Plant*

Science, 8, 1037. https://doi.org/10.3389/fpls.2017.01037.

Villalba, F., Collemare, J., Landraud, P., Lambou, K., Brozek, V., Cirer, B., et al. (2008) Improved gene targeting in Magnaporthe grisea by inactivation of MgKU80 required for non-homologous end joining. *Fungal Genetics and Biology*, 45, 68–75. https://doi.org/10.1016/j.fgb.2007.06.006.

Wang, L., Gao, W., Wu, X., Zhao, M., Qu, J., Huang, C., et al. (2018) Genome-Wide Characterization and Expression Analyses of *Pleurotus ostreatus* MYB Transcription Factors during Developmental Stages and under Heat Stress Based on de novo Sequenced Genome. *International Journal of Molecular Sciences*, 19, 2052. https://doi.org/10.3390/ijms19072052.

Wieser, J. & Adams, T.H. (1995) *fibD* encodes a Myb-like DNA-binding protein that coordinates initiation of *Aspergillus mdulans* conidiophore development. *Genes & Development*, 9, 491–502.

Yu, E.Y., Yen, W.-F., Steinberg-Neifach, O. & Lue, N.F. (2010) Rap1 in *Candida albicans* : an Unusual Structural Organization and a Critical Function in Suppressing Telomere Recombination. *Molecular and Cellular Biology*, 30, 1254–1268. https://doi.org/10.1128/MCB.00986-09.

Zhang, L., Zhang, D., Chen, Y., Ye, W., Lin, Q., Lu, G., et al. (2019) *Magnaporthe oryzae* CK2 Accumulates in Nuclei, Nucleoli, at Septal Pores and Forms a Large Ring Structure in Appressoria, and Is Involved in Rice Blast Pathogenesis. *Frontiers in Cellular and Infection Microbiology*, 9, 113. https://doi.org/10.3389/fcimb.2019.00113.

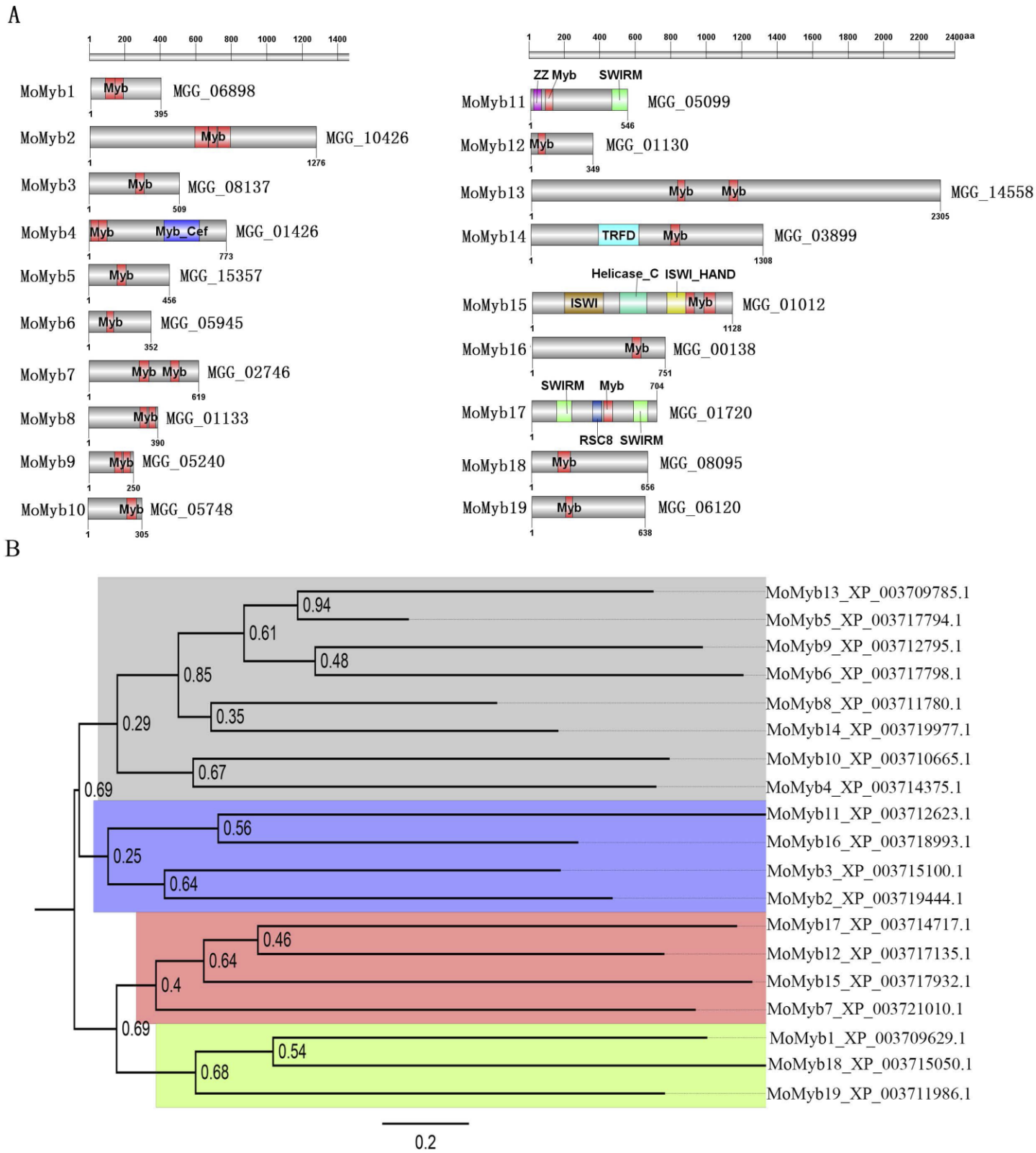

Figure 1. Domain structure of the identified genes encoding for Myb domain-containing proteins and their sequence similarities. (**A**) Identified conserved domains in the found Myb domain-containing proteins. (**B**) The similarity analysis of predicted amino acid sequences showed that the 19 proteins could be sorted into 4 groups marked by the color code.

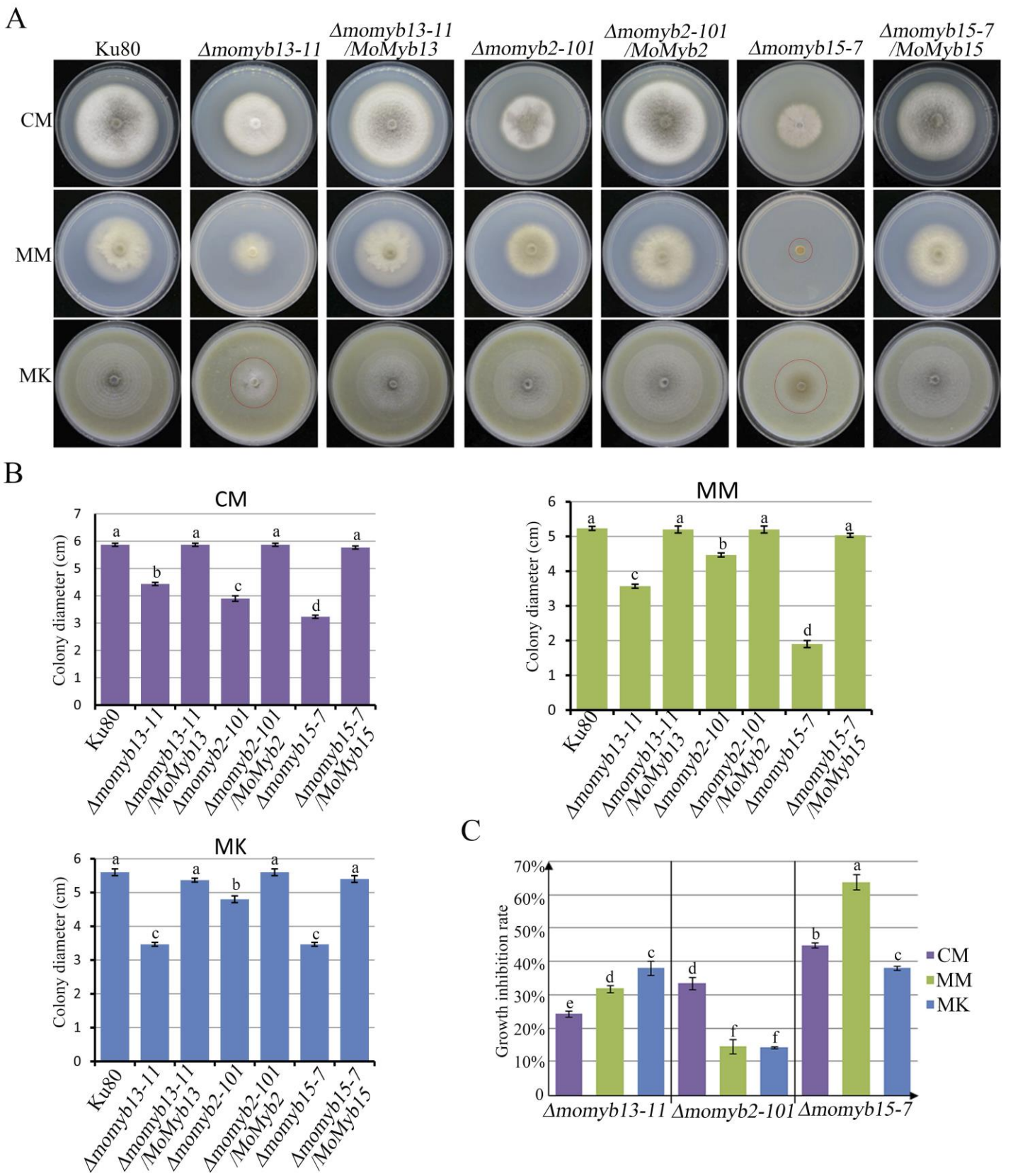

Figure 2. The radial growth rate of *Δmomyb2, Δmomyb13*, and *Δmomyb15* are slower than in the background strain Ku80. (**A**) Images of the morphology of the different strains on the three different media, complete medium (CM), minimal medium (MM), and rice bran medium (RBM). (**B**) Measured colony diameter after 10day incubation in alternating dark/light (12h/12h) at 25 ^{O}C. (**C**) Growth inhibition in deletion strains was measured as colony diameter after 10-day incubation in alternating dark/light (12h/12h) at 25 ^{O}C compared to the background strain Ku80. Bars indicate SEM and bars with the same letters are not significantly different (P>0.05; t-test).

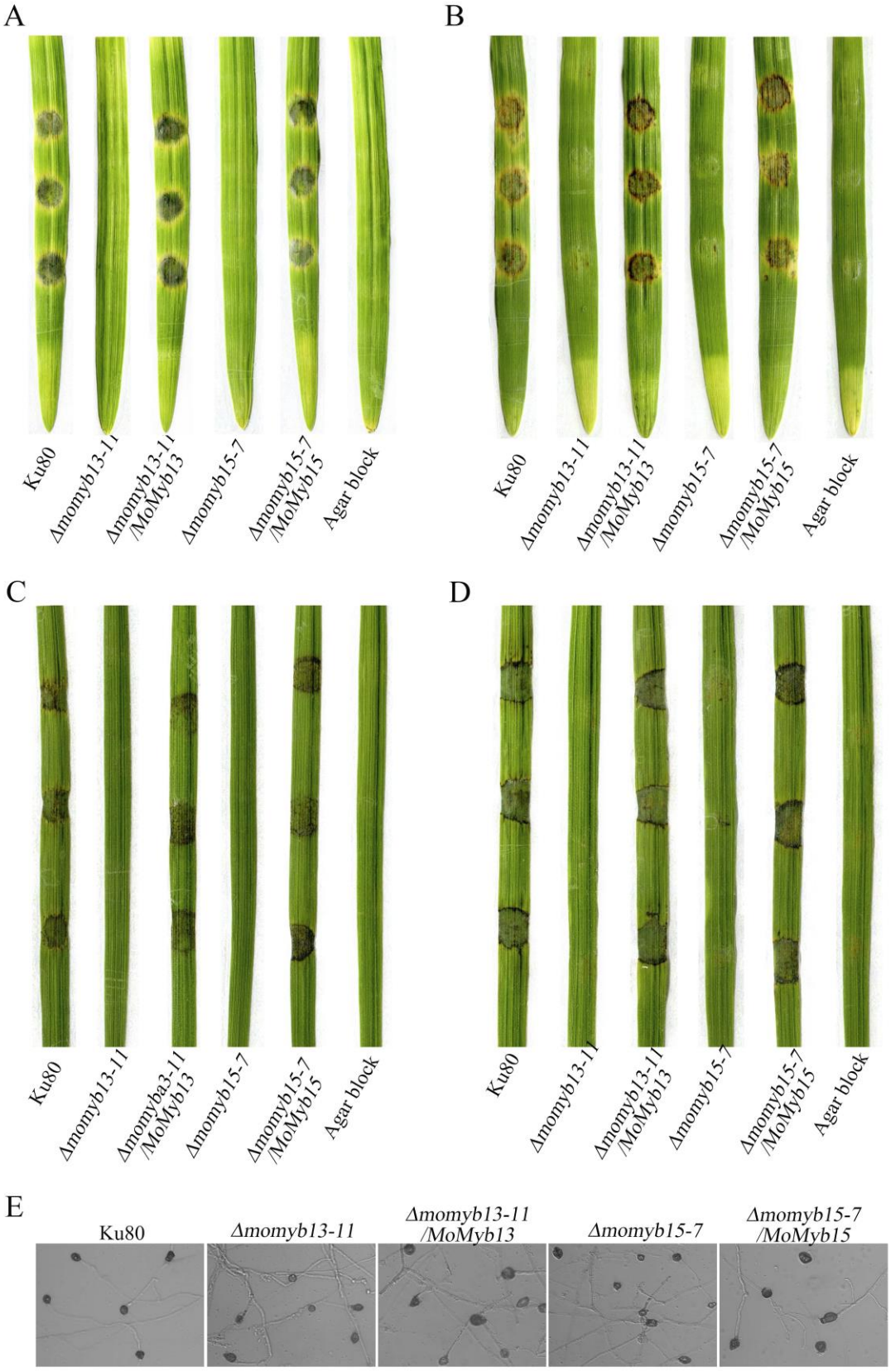

Figure 3. MoMyb13 and MoMyb15 are involved in M. oryzae pathogenicity since mutants of the genes showed reduced lesions when tested with the agar block technique on excised barley and rice leaves, but this lack of lesion is not the result of lack of mycelia appressorium formation. Test of mutants and background strain on intact (**A**) and wounded (**B**) barley leaves. Test of mutants and background strain on intact (**C**) and wounded (**D**) rice leaves. Mycelia appressorium formation from mycelial fragments on a hydrophobic surface (**E**).

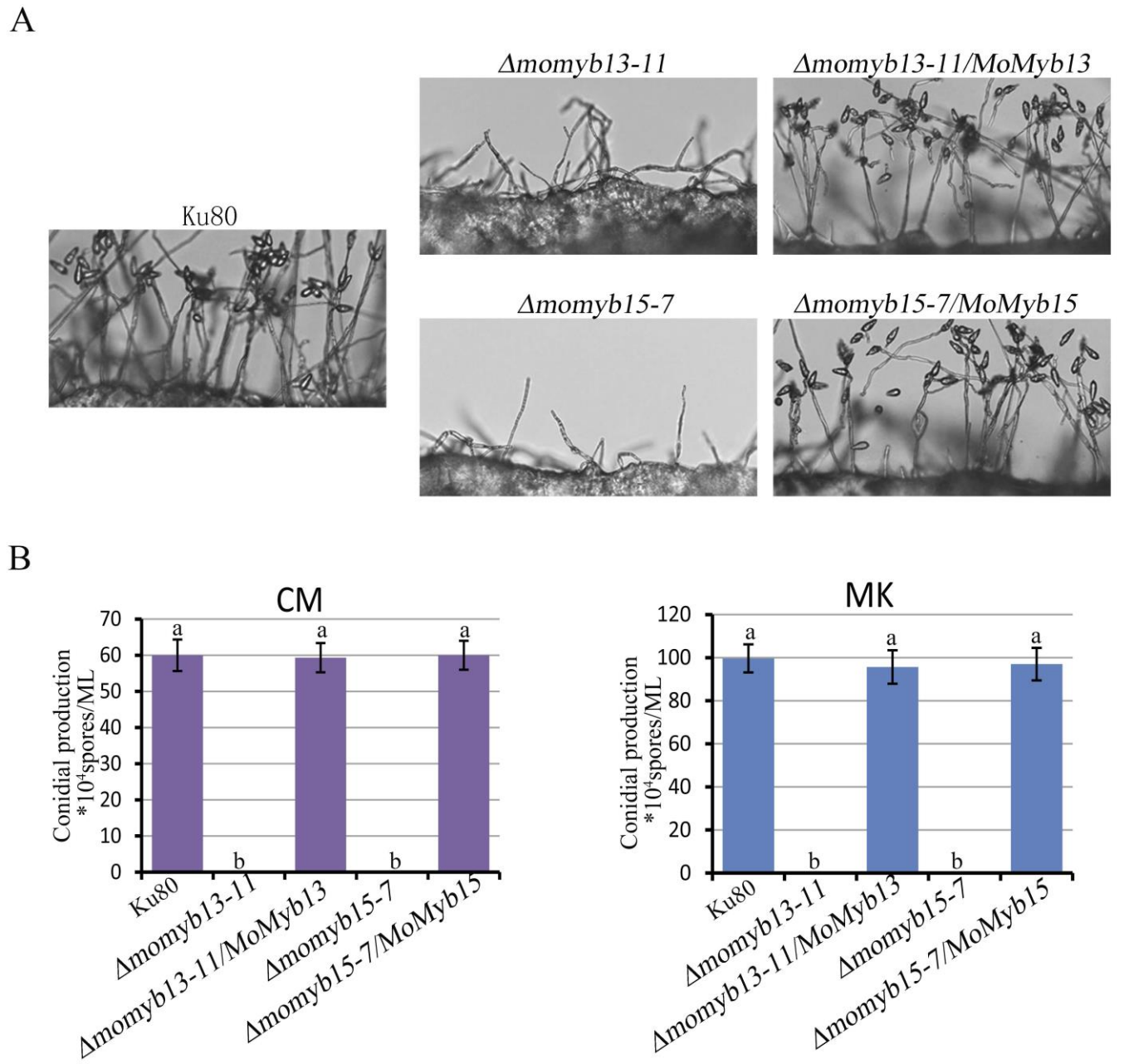

Figure 4. Δmomyb13 and Δmomyb15 make no conidia, while Ku80 and complement strains readily make. (**A**) Conidiophore morphology and conidiation. (**B**) Conidia production on CM and RBM. Bars with the same letters are not significantly different (P>0.05).

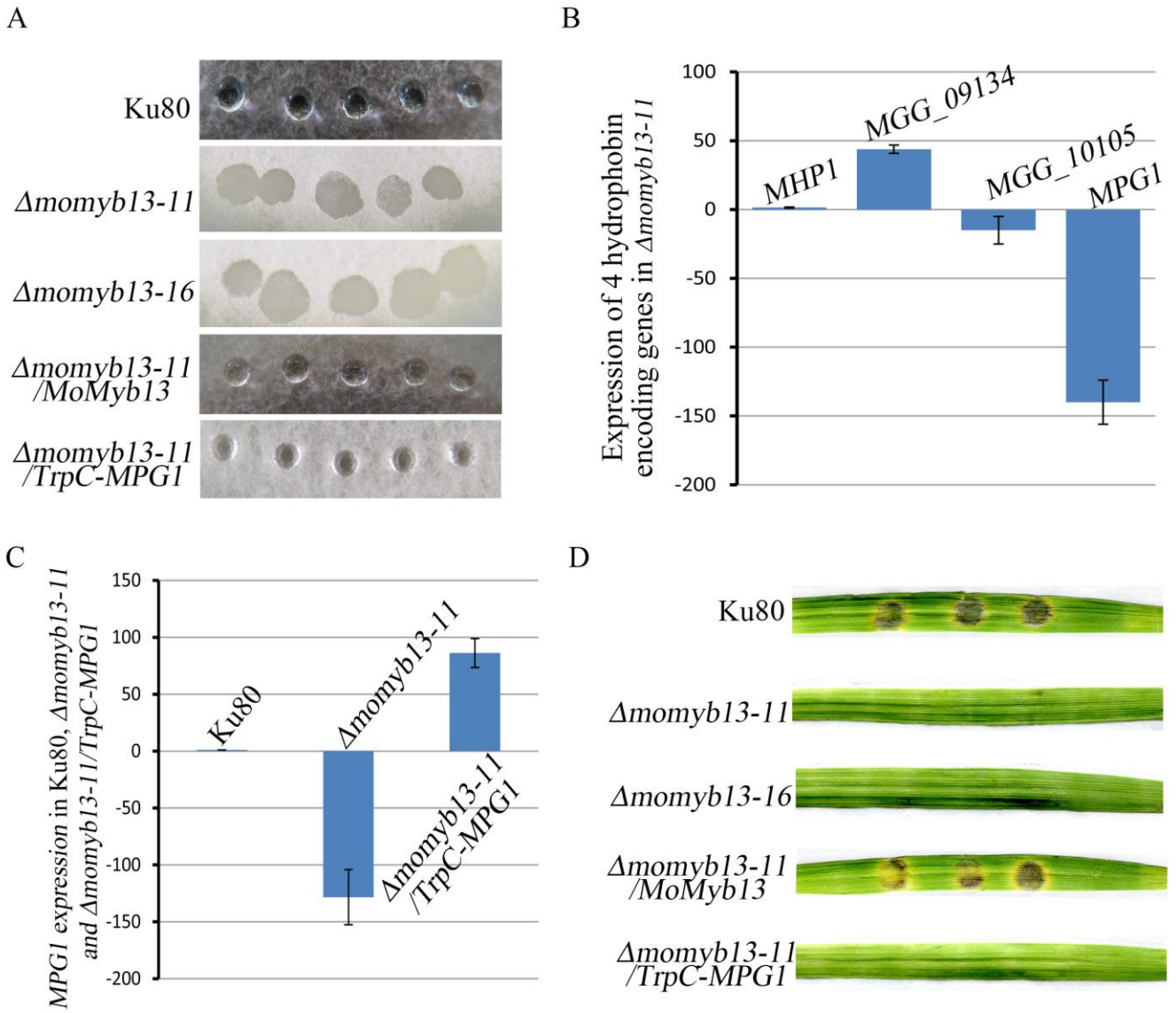

Figure 5. Hydrophobin production, necessary for producing hydrophobic aerial conidia-producing mycelium, by MPG1 is downregulated in *Δmomyb13*, but overexpression of the *MPG1* gene in the *Δmomyb13* strain does not restore pathogenicity. (A) colonies of *Δmomyb13* are easily wettable, while the surface of the background strain (*Ku80*), the complementation strain, or the *Δmomyb13* strain containing the overexpressed hydrophobin MPG1 (*Δmomyb13-11/TrpC-MPG1*) is not wettable. (B) Percent change in expression of 4 hydrophobin genes in *Δmomyb13* h compared to Ku80, showing that MPG1 is severely downregulated while the others are less affected. (C) Percent change in *MPG1* expression in *Ku80*, *Δmomyb13* and *Δmomyb13/TrpC-MPG1* strains compared to *Ku80*. (D) Leaf lesions formed by the *Ku80*, *Δmomyb13*, and *Δmomyb13/TrpC-MPG1* strains using the agar block technique. Error bars in (A) and (C) show the 95% confidence intervals. Bars with confidence intervals not overlapping with other bars' confidence intervals or levels (as zero) are significantly different (P<0.05 for the null hypothesis that they are the same).

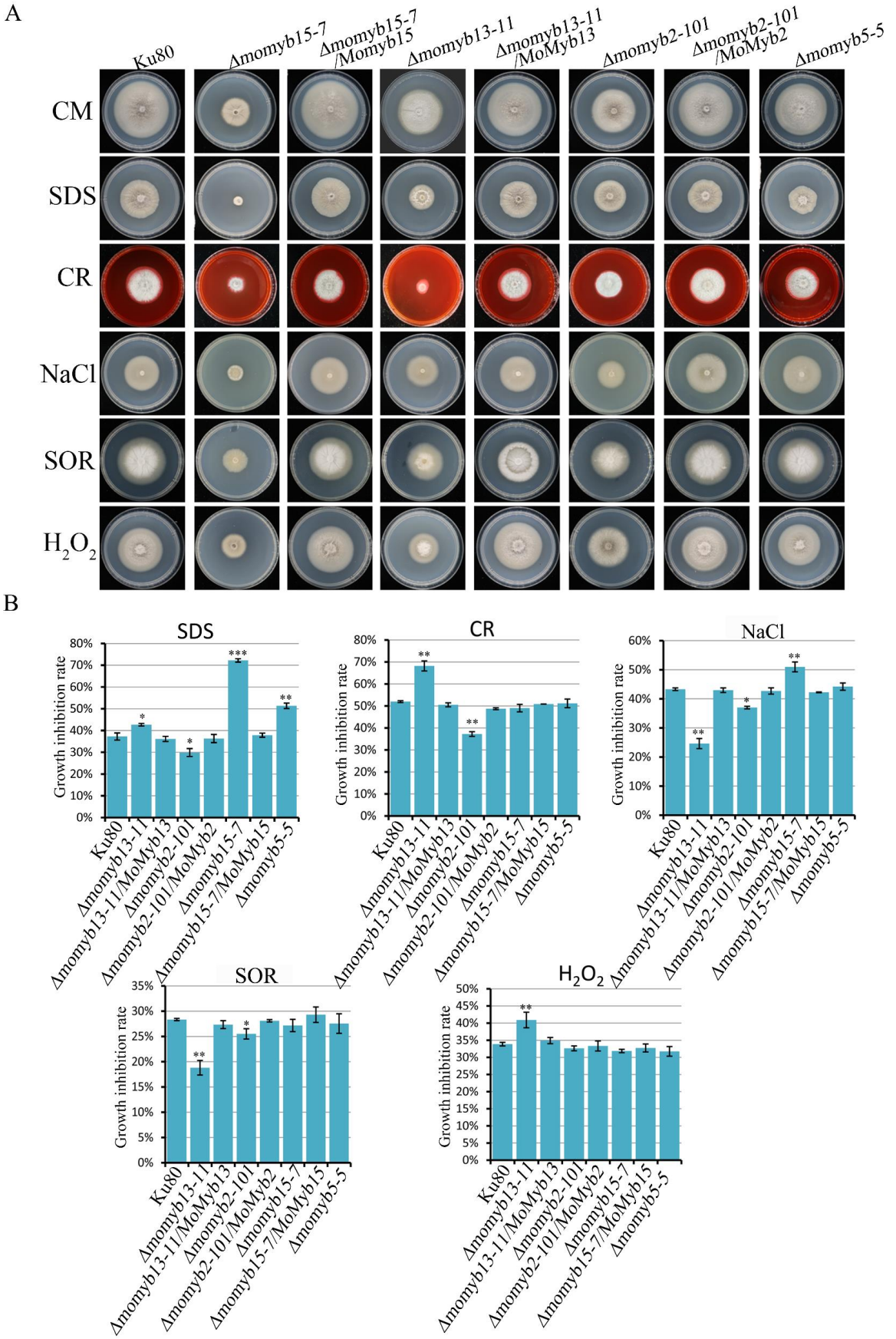

Figure 6. The three mutants, Δmomyb5, Δmomyb13, and Δmomyb15, showed reduced stress tolerance compared to the background strain Ku80 using a standard panel of stress treatments. (**A**) Colony size and morphology of Ku80, the mutants, and the complements after 10 days in alternating dark/light (12h/12h) at 25ºC growing on CM or CM with additions of SDS, CR, NaCl SOR, or H_2O_2 as stresses (see methods). (**B**) Same as in (**A**) but shows the average of 3 replicates with error bars. Error bars show the standard error of the respective averages, and stars mark statistical differences compared to Ku80.

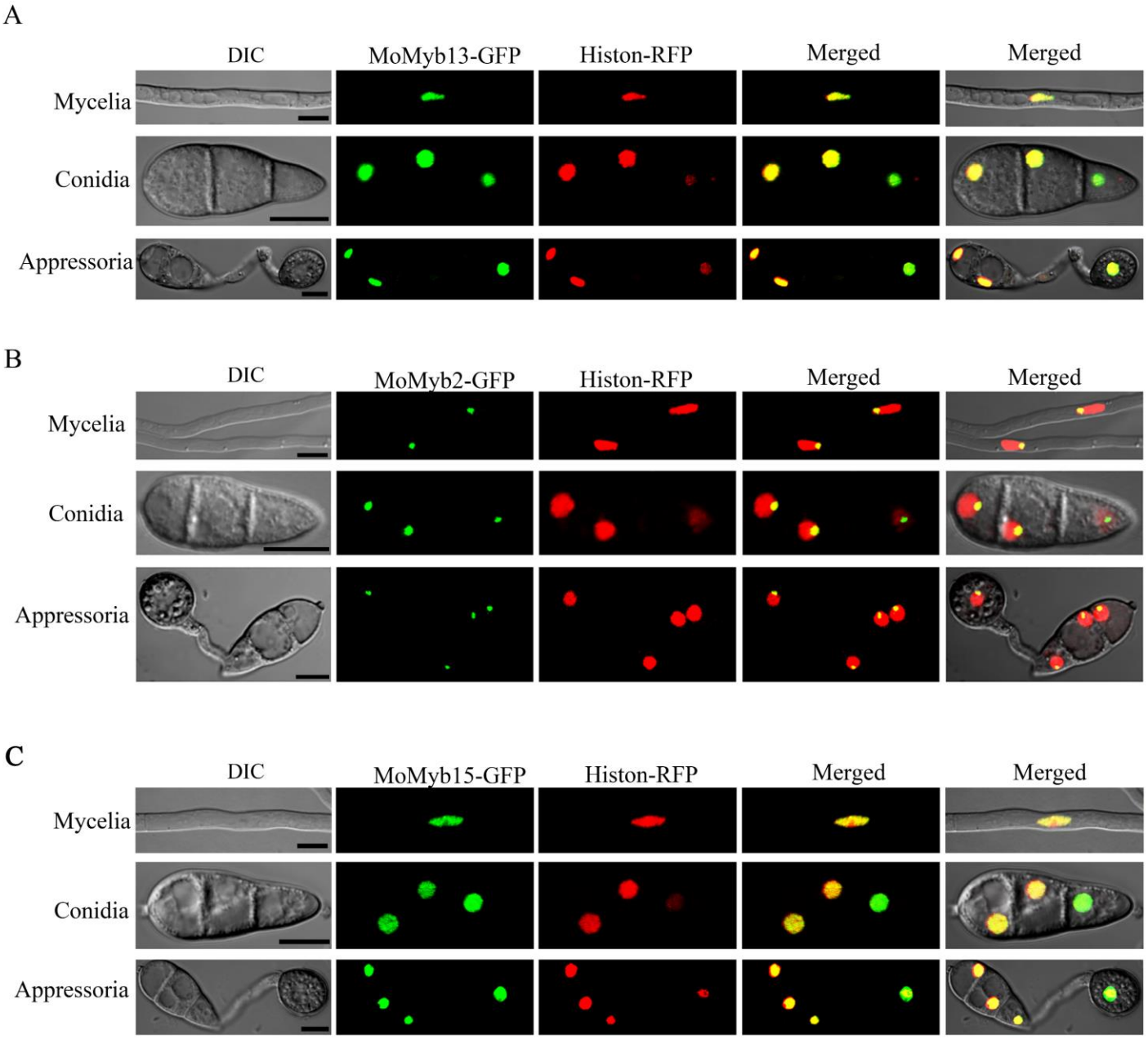

Figure 7. All three *momyb*-deletions that showed phenotypes differing from Ku80 (*Δmomyb13*, *Δmomyb2*, and *Δmomyb15*) localize to conidia, appressorial, and mycelial nuclei as indicated by co-localization with the mCherry labeled nuclear marker MoHis1-mCherry confirming that they are indeed localized to nuclei as expected. **(A**) MoMyb13-GFP localizes to nuclei. (**B**) MoMyb2-GFP localizes to nuclei but mainly to what is most probably the nucleoli. (**C**) MoMyb15-GFP localizes to nuclei. DIC= Differential Interference Contrast.

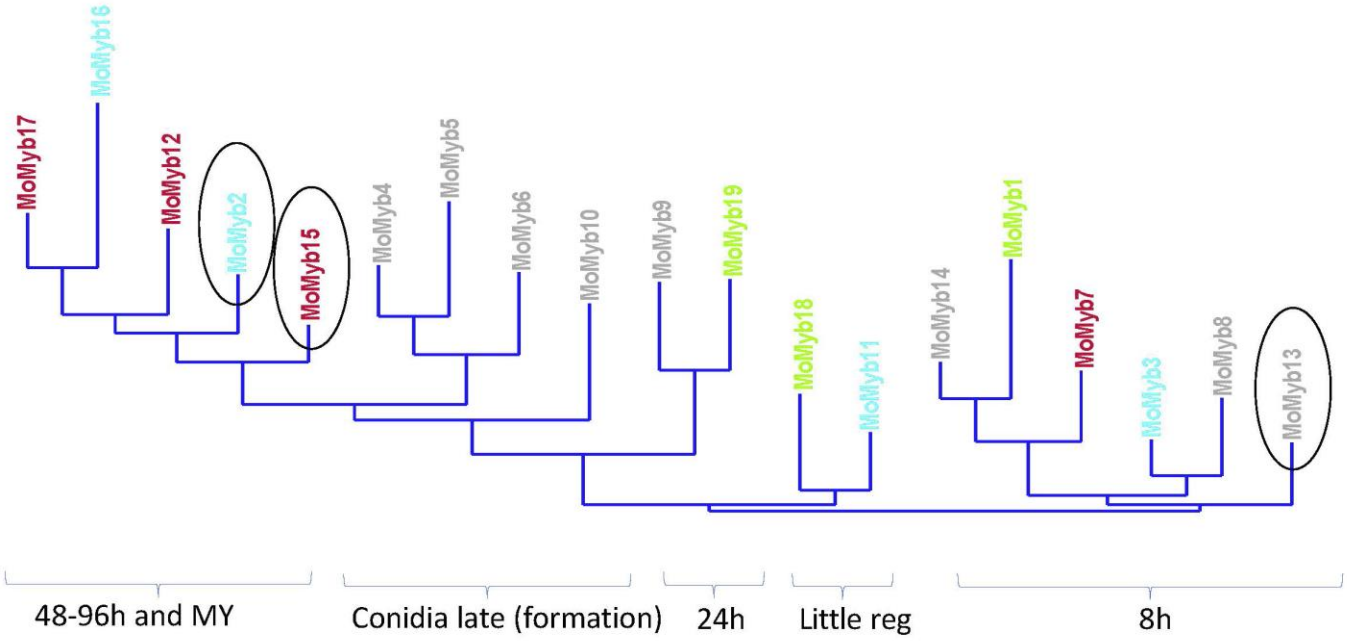

Figure 8. The different *MoMyb* genes show different expression profiles. The expression profiles cluster into 5 groups depending on hours post-infection (HPI) expression during infection. This clustering is, in principle, similar to what can be seen in the PCA plot (**Fig. S5**). Transcripts from growth on agar medium (MY), conidia (late in the formation of conidia), and in rice plant leaves at 8 HPI (8h), 24 HPI (24h), 48 HPI (48h), 72 HPI (72h), and 96 HPI (96h). The color code used is the same as in **Fig. 1B** for the phylogeny clusters showing that the regulatory sub-clusters activated at different HPI contain sets of genes with little similarity in sequence homology. Ellipses mark the 3 genes with phenotypes different from Ku80 for their respective deletion mutants.

Table 1. Phenotype summary of MoMybs.

Protein name	Gene ID	Deletion	Growth	Conidiation	Appressoria formation	Pathogenicity	localization	Stress response	Ref
MoMyb1	MGG_06898	Yes	Reduced	Lost	Reduced	Reduced	cytoplasm and nucleus	Less sensitive to salt and sorbitol	Dong et al., 2015; Lee et al., 2021
MoMyb2	MGG_10426	Yes	Reduced	Normal	Normal	Normal	nucleolus	More sensitive to SDS	This study; Lee et al., 2021
MoMyb3	MGG_08137	Yes	Normal	Normal	Normal	Normal	-	-	This study; Lee et al., 2021
MoMyb4	MGG_01426	Yes	Normal	Normal	Normal	Normal	nucleus	-	This study; Lee et al., 2021
MoMyb5	MGG_15357	Yes	Normal	Normal	Normal	Normal	nucleus	-	This study; Lee et al., 2021
MoMyb6	MGG_05945	Yes	Normal	Normal	Normal	Normal	-	-	This study; Lee et al., 2021
MoMyb7	MGG_02746	Yes	Normal	Normal	Normal	Normal	-	-	Lee et al., 2021
MoMyb8	MGG_01133	Yes	Normal	Normal	Normal	Normal	-	-	This study; Lee et al., 2021
MoMyb9	MGG_05240	Yes	Normal	Normal	Normal	Normal	nucleus	-	This study; Lee et al., 2021
MoMyb10	MGG_05748	Yes	Normal	Normal	Normal	Normal	-	-	This study
MoMyb11	MGG_05099	Not	-	-	-	-	nucleus	-	This study
MoMyb12	MGG_01130	Not	-	-	-	-	-	-	This study
MoMyb13	MGG_14558	Yes	Reduced	Lost	Normal	Lost	nucleus	More sensitive to CR and H_2O_2; Less sensitive to NaCl and SOR	This study
MoMyb14	MGG_03899	Yes	Normal	Normal	Normal	Normal	-	-	This study
MoMyb15	MGG_01012	Yes	Reduced	Lost	Normal	Lost	nucleus	More sensitive to SDS	This study
MoMyb16	MGG_00138	Yes	Normal	Normal	Normal	Normal	nucleus	-	This study
MoMyb17	MGG_01720	Not	-	-	-	-	nucleus		This study
MoMyb18	MGG_08095	Yes	Normal	Normal	Normal	Normal	nucleus	-	This study
MoMyb19	MGG_06120	Not	-	-	-	-	-	-	This study

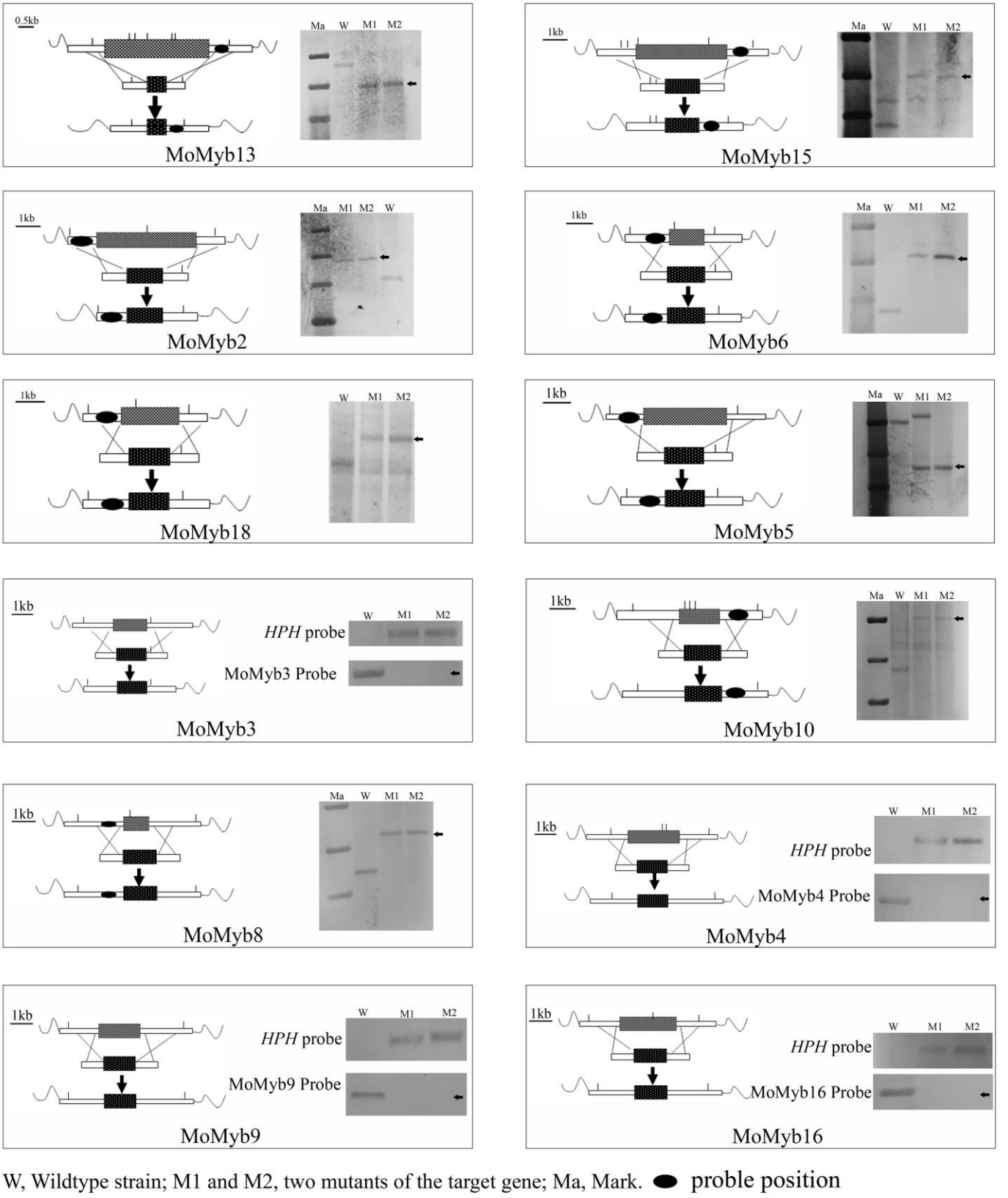

Figure S1. Southern blot confirmation for all the 12 mutants obtained in this study. The HPH gene or the 1.0 kb up- or downstream of the target gene was used as a probe to detect successful gene knockout events.

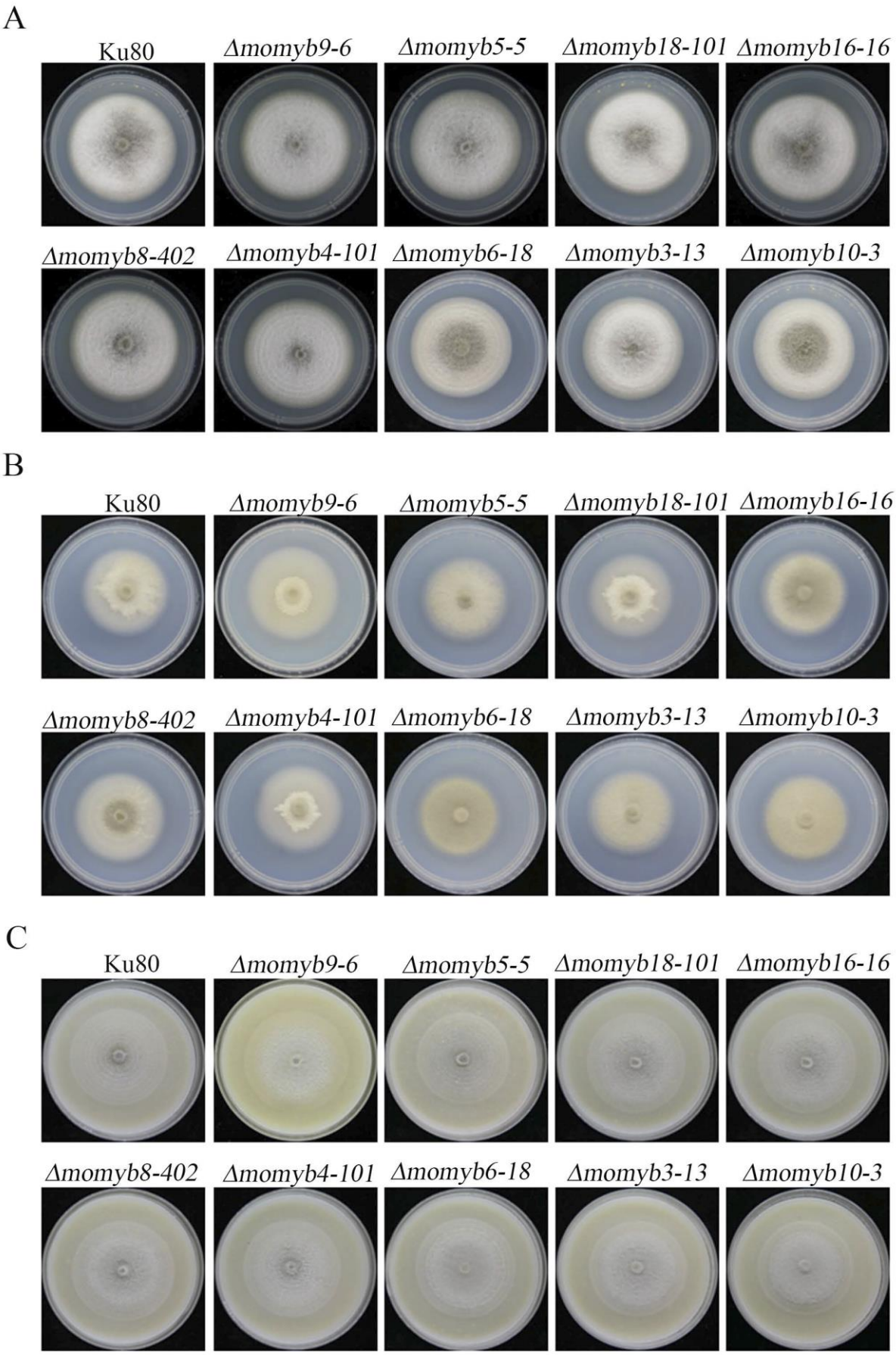

Figure S2. Colony morphology of the 9 Myb gene mutants with no effect on pathogenicity compared to Ku80 on CM (**A**) MM **(B**), and RBM (**C**).

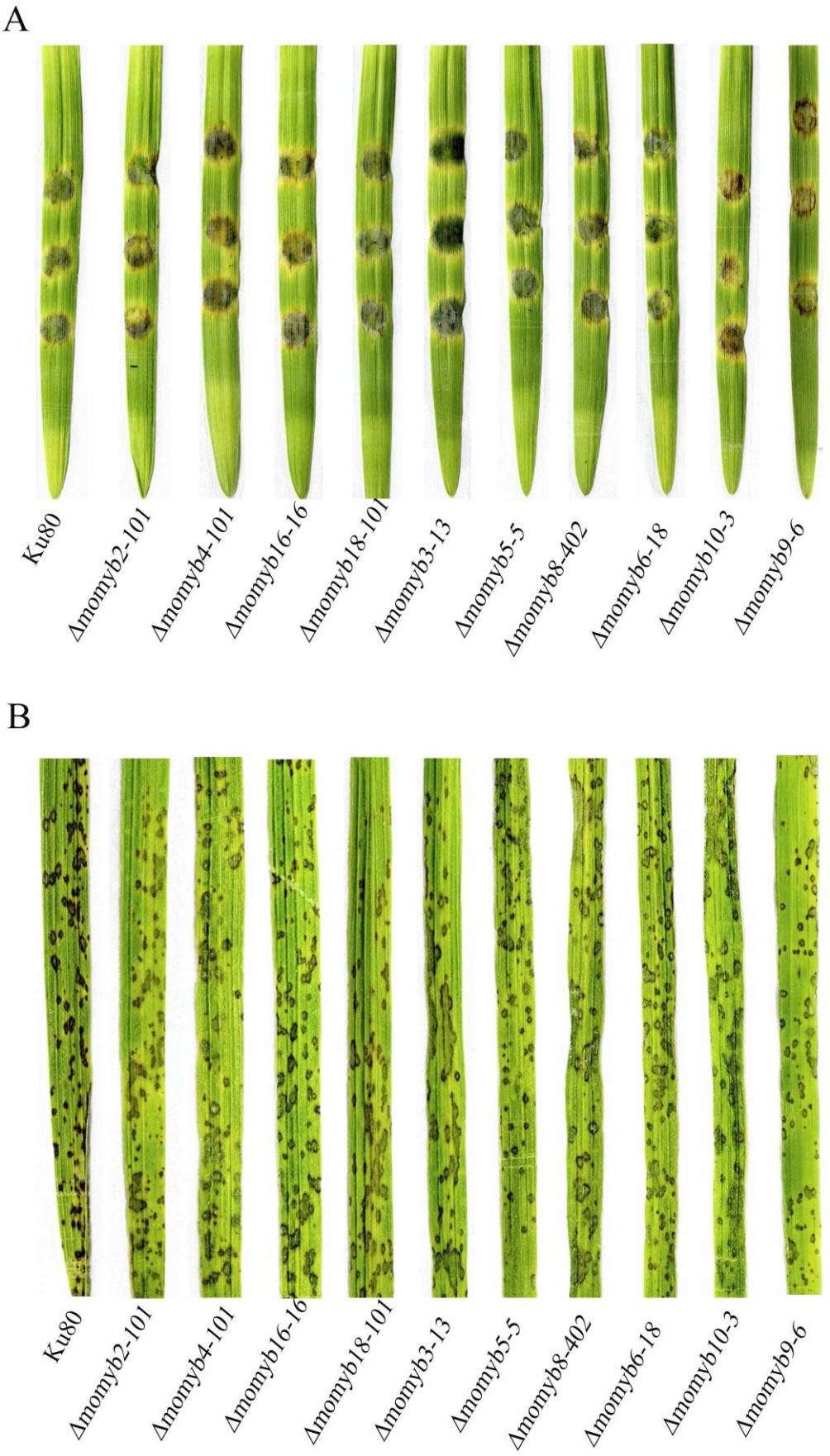

Figure S3. No effect on pathogenicity due to the Myb gene mutations can be seen for 9 mutants tested using either the agar block technique or conidia sprayed on the leaves. (**A**) Test of mutants and background strain (Ku80) on barley leaves using the agar block technique (**B**) Test of mutants and background strain (Ku80) conidia sprayed on rice leaves.

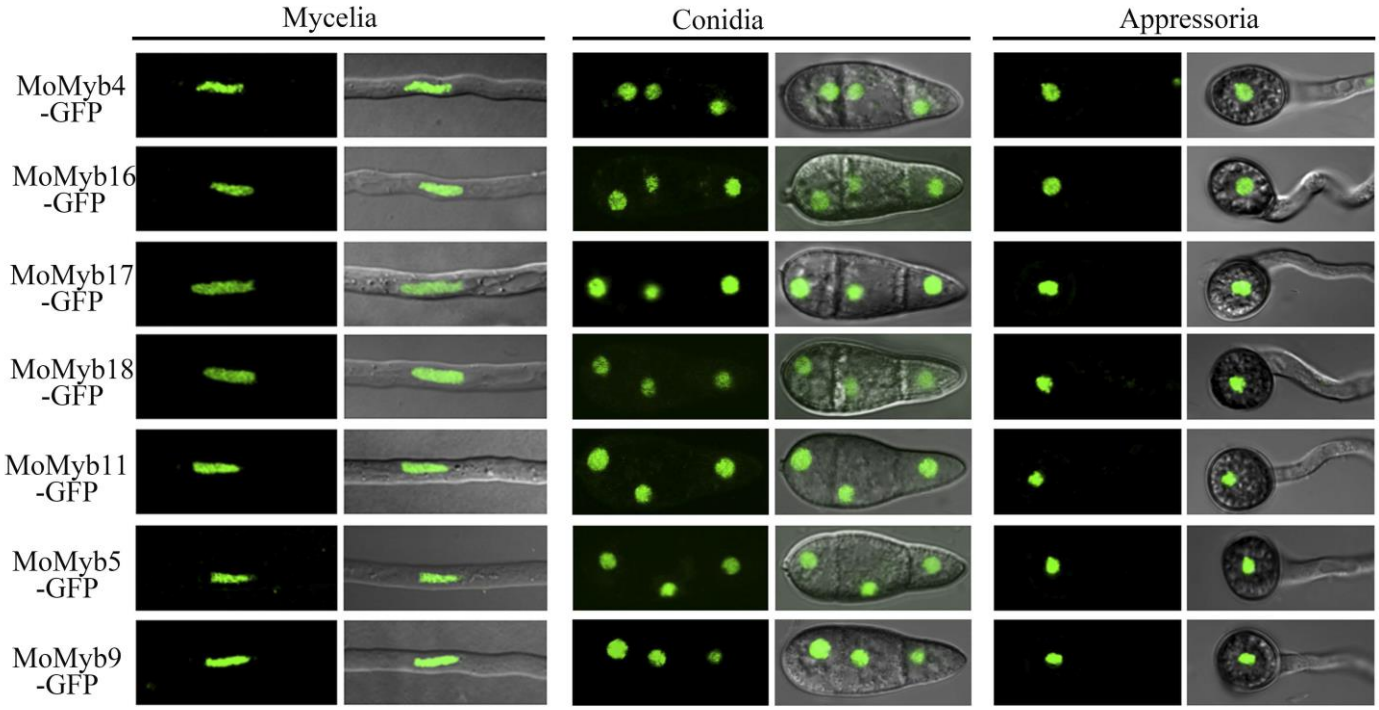

Figure S4. Localization of the MoMyb-GFP complements from which we could find strong enough GFP signals in mycelia conidia and appressoria. The localization pattern suggests nuclear localisations as expected for Myb-domain-containing proteins.

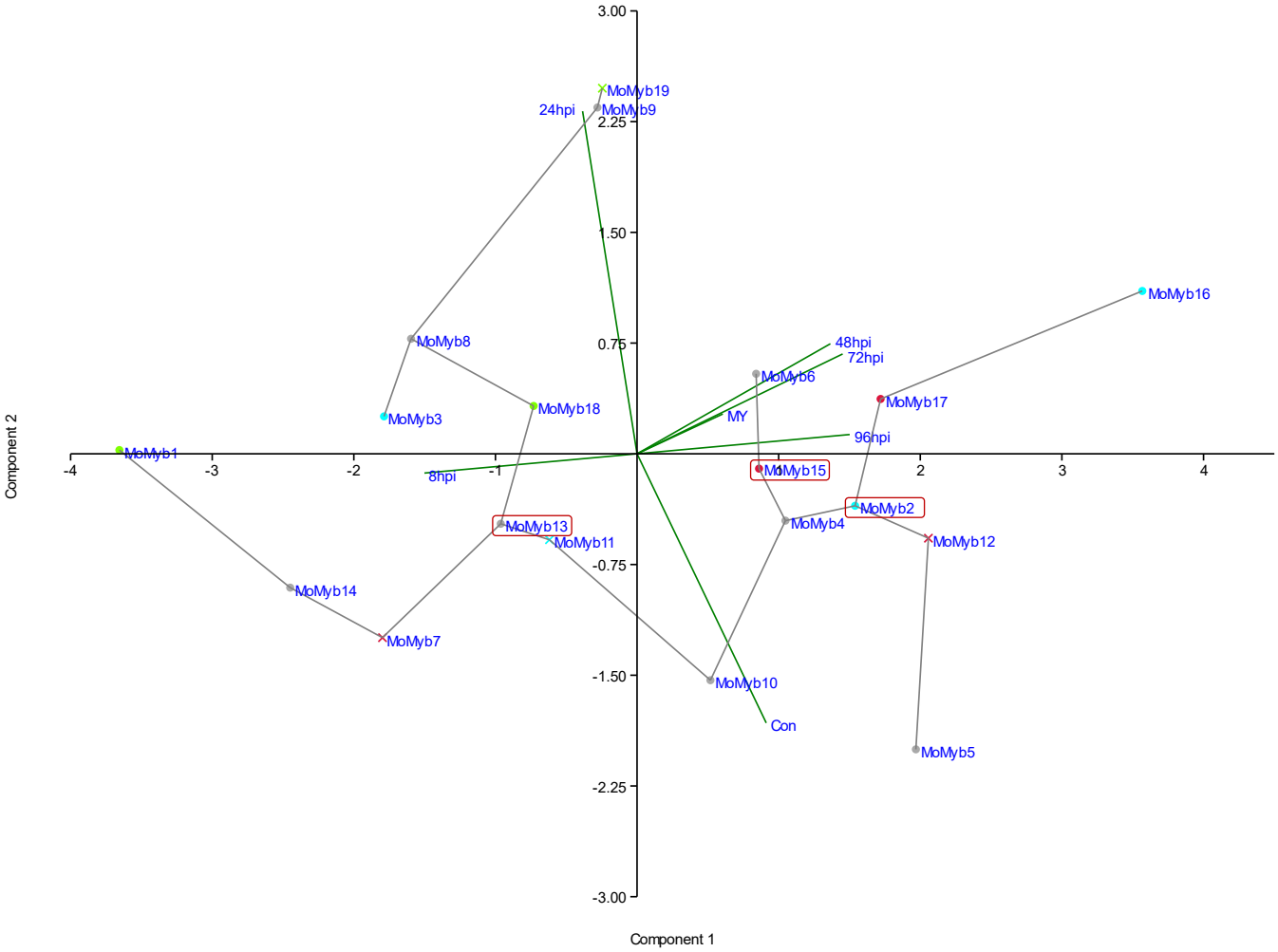

Figure S5. The *MoMyb* genes show different expression profiles visualized by Principal Component Analysis (PCA). Variables were transcription with different treatments and HPIs from infected rice leaves, growth on agar medium (MY), conidia (Conidia late), 8 HPI (8h), 24 HPI (24h), 48 HPI (48h), 72 HPI (72h) and 96 HPI (96h). The expression values of the 19 identified genes encoding Myb domain-containing proteins were the objects. The first and second PCA are presented after a PCA based on the correlation of the expression profiles (as shown in **Table S2**). The plot is a biplot also showing the loading of the variables in the two PCs. A "Minimum spanning tree" nearly identical to the tree in Fig. 8 joins the most similar expressed genes for all calculated PCs. The color code used for the marker dots (or Xs) in front of the gene names is the same as in **Fig. 1B** for the predicted amino acid sequence similarity clusters, showing that the regulatory clusters contain sets of genes with little similarity in sequence homology. A marker X in front of the gene name shows a gene we could not delete. Boxes mark the 3 genes with noted phenotypes for their deletion mutants. MoMyb1, furthest to the left in the figure, is known from the literature to be activated early in infection, and here it is far left in component 1 with the 8 HPI negative loading corroborating the previous results from the literature.

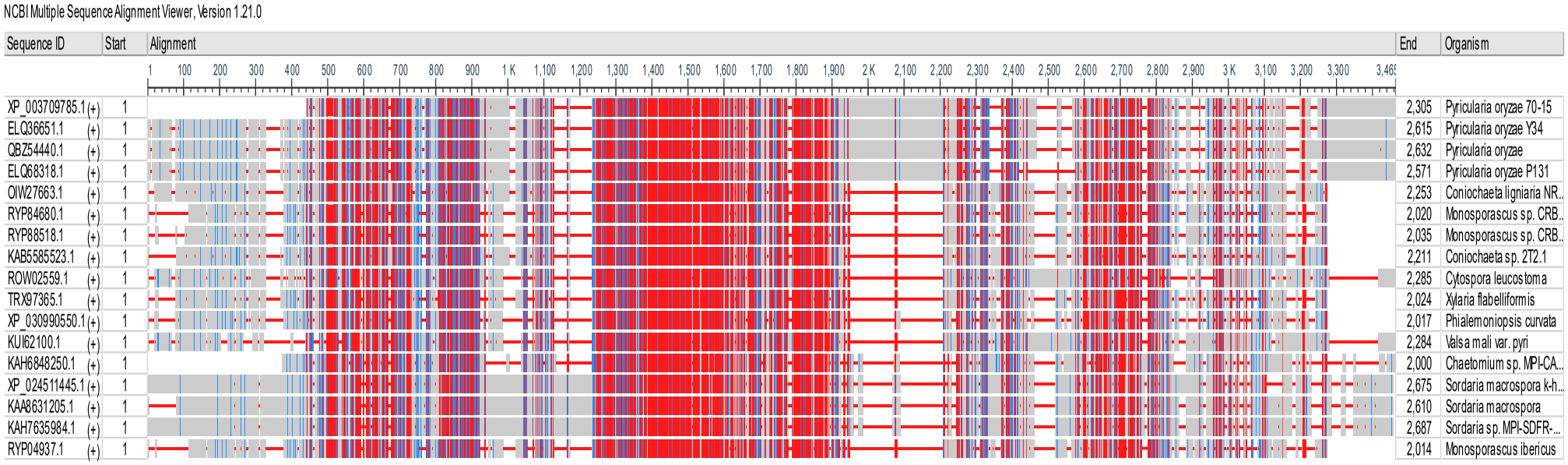

Figure S6. Alignments of the most similar orthologues to the MoMyb13 protein from species related to *M. oryzae* (*Pyricularia oryzae*)(all are with E-values less or equal to 3E-135 and with more than 70% query cover) (**Table S3**). Data from an NCBI produced by the alignment of all fungal genomes annotated.

Table S1. Primers used in this study, their sequences, and what they were used to accomplish.

Protein name	Gene ID	Deletion	Growth	Conidiation	Appressoria formation	Pathogenicity	localization	Stress response	Ref
MoMyb1	MGG_06898	Yes	**Reduced**	**Lost**	**Reduced**	**Reduced**	cytoplasm and nucleus	Less sensitive to salt and sorbitol	Dong et al., 2015; Lee et al., 2021
MoMyb2	MGG_10426	Yes	**Reduced**	Normal	Normal	Normal	nucleolus	More sensitive to SDS	This study; Lee et al., 2021
MoMyb3	MGG_08137	Yes	Normal	Normal	Normal	Normal	-	-	This study; Lee et al., 2021
MoMyb4	MGG_01426	Yes	Normal	Normal	Normal	Normal	nucleus	-	This study; Lee et al., 2021
MoMyb5	MGG_15357	Yes	Normal	Normal	Normal	Normal	nucleus	-	This study; Lee et al., 2021
MoMyb6	MGG_05945	Yes	Normal	Normal	Normal	Normal	-	-	This study; Lee et al., 2021
MoMyb7	MGG_02746	Yes	Normal	Normal	Normal	Normal	-	-	Lee et al., 2021
MoMyb8	MGG_01133	Yes	Normal	Normal	Normal	Normal	-	-	This study; Lee et al., 2021
MoMyb9	MGG_05240	Yes	Normal	Normal	Normal	Normal	nucleus	-	This study; Lee et al., 2021
MoMyb10	MGG_05748	Yes	Normal	Normal	Normal	Normal	-	-	This study
MoMyb11	MGG_05099	Not	-	-	-	-	nucleus	-	This study
MoMyb12	MGG_01130	Not	-	-	-	-	-	-	This study
MoMyb13	MGG_14558	Yes	**Reduced**	**Lost**	Normal	**Lost**	nucleus	More sensitive to CR and H_2O_2; Less sensitive to NaCl and SOR	This study
MoMyb14	MGG_03899	Yes	Normal	Normal	Normal	Normal	-	-	This study
MoMyb15	MGG_01012	Yes	**Reduced**	**Lost**	**Normal**	**Lost**	nucleus	More sensitive to SDS	This study
MoMyb16	MGG_00138	Yes	Normal	Normal	Normal	Normal	nucleus	-	This study
MoMyb17	MGG_01720	Not	-	-	-	-	nucleus		This study
MoMyb18	MGG_08095	Yes	Normal	Normal	Normal	Normal	nucleus	-	This study
MoMyb19	MGG_06120	Not	-	-	-	-	-	-	This study

"-"means not assayed.

Table S1. Primers used in this study

Name	Sequences	Application
MGG_01720-UP-F	aagggaacaaaagctggtaccttctctgggagaccctgttg	Gene deletion
MGG_01720-UP-R	tcagttaacgtcgacaagctttgtggttgtagggtgtcgaa	Gene deletion
MGG_01720-down-F	cgggaaccagttaacctgcagtttgcactacgtcagggaga	Gene deletion
MGG_01720-down-R	cgctctagaactagtggatcccgcttacagtgcttgttgga	Gene deletion
MGG_01012-UP-F	aagggaacaaaagctggtaccACGGCTTGACGGTTACTTGT	Gene deletion
MGG_01012-UP-R	tcagttaacgtcgacaagcttTTGTCGTGAGATTCCCTGGT	Gene deletion
MGG_01012-down-F	cgggaaccagttaacctgcagGTTTGGAACTCTTTGATGGG	Gene deletion
MGG_01012-down-R	cgctctagaactagtggatccGGGCTACTTTGACTTTATGT	Gene deletion
pCB1532-MGG_01012-Pro-F	cgctctagaactagtggatccAGGTGGATGATGTCGATTGCC	Gene complementation
pCB1532-MGG_01012-EcoR1	gcccttgctcaccatgaattcTTTCTTCTTGCCCTTGGCC	Gene complementation
MGG_00138-UP-F	aagggaacaaaagctggtaccCGTTGAGCCTGCGGTTTTAT	Gene deletion
MGG_00138-Up-R	tcagttaacgtcgacaagcttGAAGGTGGCGGTCTGTTTGT	Gene deletion
MGG_00138-down-F	cgggaaccagttaacctgcagTGGCATTGGCGTTTGTTGAG	Gene deletion
MGG_00138-down-R	cgctctagaactagtggatccCAGGAGCATTATTGCGTGGG	Gene deletion
MGG_01426-UP-F	aagggaacaaaagctggtaccGCTGGAGCGGCTTTGTTTGG	Gene deletion
MGG_01426-UP-R	tcagttaacgtcgacaagcttTGGAGATGAGCGGCGACTGG	Gene deletion
MGG_01426-DW-F	cgggaaccagttaacctgcagCAAACGAGAAGAAGGGGAAG	Gene deletion
MGG_01426-DW-R	cgctctagaactagtggatccGCGCACTATGAAAGGAAGCT	Gene deletion
MGG_08095-UP-F	aagggaacaaaagctggtaccGAACAAAGTTGAAAAGAGCG	Gene deletion
MGG_08095-UP-R	tcagttaacgtcgacaagcttAAATCCTGGATAATCGAGCA	Gene deletion
MGG_08095-DW-F	cgggaaccagttaacctgcagTATAATTCATGAGGCCACCT	Gene deletion
MGG_08095-DW-R	cgctctagaactagtggatccCTATTCTTCTCCCTTTTGCT	Gene deletion
MGG_02746-UP-F	aagggaacaaaagctggtaccGTAAGTAAGGTGTAGGAGCG	Gene deletion
MGG_02746-UP-R	tcagttaacgtcgacaagcttCGACTAATAAGAAAGCGGAG	Gene deletion
MGG_02746-DW-F	cgggaaccagttaacctgcagTGGGGAGAACTTTGTGTGGA	Gene deletion
MGG_02746-DW-R	cgctctagaactagtggatccTTGAGGGTCAGGGTTGAGGA	Gene deletion
pCB1532-MG02746- BamH1-F	cgctctagaactagtggatccCCGTAGTCAATTGTGTCGC	Gene complementation
pCB1532-MG02746-EcoR1-R	gcccttgctcaccatgaattcTTTCTGCGTGTCGTCTAGAAGC	Gene complementation
MGG_03899-UP-F:	aagggaacaaaagctggtaccCAAATGAAGCAGCGGACAGC	Gene deletion
MGG_03899-UP-R	tcagttaacgtcgacaagcttACCATAGAAATTACCAGGAA	Gene deletion
MGG_03899-DW-F	cgggaaccagttaacctgcagGTTATATGGTGTTTTAGGAG	Gene deletion
MGG_03899-DW-R	cgctctagaactagtggatccGGAAGTTGTTGAATTTAGTG	Gene deletion

MGG_10426-UP-F	aagggaacaaaagctggtaccGAATAACAACCAACTCCTCC	Gene deletion
MGG_10426-UP-R	tcagttaacgtcgacaagcttCATAAAATCCGTTTCTCAGC	Gene deletion
MGG_10426-DW-F	cgggaaccagttaacctgcagGCTTTGCTCGGTGTTGATTT	Gene deletion
MGG_10426-DW-R	cgctctagaactagtggatccCTTTGGTTGATGCCTCCTGT	Gene deletion
pCB1532-MGG_10426-BamH1-F	cgctctagaactagtggatccAACAGCCTACGACATCCCAAG	Gene complementation
pCB1532-MGG_10426-EcoR1-R	gcccttgctcaccatgaattcCTGCTCGATCGTCATTTGACT	Gene complementation
MGG_05099-UP-F	aagggaacaaaagctggtaccAATGTCTTCTCGTATTTCGG	Gene deletion
MGG_05099-UP-R:	tcagttaacgtcgacaagcttTGGTAGTCGTGTAGCTGTTT	Gene deletion
MGG_05099-DW-F	cgggaaccagttaacctgcagTCGGGCGTGTACTAGGGATA	Gene deletion
MGG_05099-DW-R	cgctctagaactagtggatccCCAACTTTGGAAAGTTTGGC	Gene deletion
MGG_05945-UP-F	aagggaacaaaagctggtaccGTTGGGGTTTTTGGTTGTTT	Gene deletion
MGG_05945-UP-R	tcagttaacgtcgacaagcttGGTTTGGCACTCTCGTCTTA	Gene deletion
MGG_05945-DW-F	cgggaaccagttaacctgcagCGCACCTGACCCGAAACAAC	Gene deletion
MGG_05945-DW-R	cgctctagaactagtggatccTCCTCATGCCGACAAATGAA	Gene deletion
MGG_05240-UP-F	aagggaacaaaagctggtaccTGCTGCTTTCAATCTTGTTC	Gene deletion
MGG_05240-UP-R	tcagttaacgtcgacaagcttGATGGGCGTGATGCTCCGTG	Gene deletion
MGG_05240-DW-F	cgggaaccagttaacctgcagCACATGAATCATCCCACACC	Gene deletion
MGG_05240-DW-R	cgctctagaactagtggatccCAAAGCAACAGTCACTACCG	Gene deletion
MGG_06120-UP-F	aagggaacaaaagctggtaccGGGCAGCCTGCTCCACGAGT	Gene deletion
MGG_06120-UP-R	tcagttaacgtcgacaagcttATGGGAAGATGGGCGATTTT	Gene deletion
MGG_06120-DW-F	cgggaaccagttaacctgcagGTCCGTGCGTGTCCGTCTCT	Gene deletion
MGG_06120-DW-R	cgctctagaactagtggatccCGCGGTGCAGCTGATTTTTT	Gene deletion
MGG_01133-UP-F	aagggaacaaaagctggtaccAGTTCATCTTGTGCTTGGGG	Gene deletion
MGG_01133-UP-R	tcagttaacgtcgacaagcttCGTTGGTGTGTACCTTTTGG	Gene deletion
MGG_01133-DW-F	cgggaaccagttaacctgcagCACTTTTTTTATACTGCGCT	Gene deletion
MGG_01133-DW-R	cgctctagaactagtggatccATCTTTTACCTGTTACGACC	Gene deletion
pCB1532-MGG_01133-BamH1-F	cgctctagaactagtggatccGGAGAATAGCGGCTAGACCT	Gene complementation
pCB1532-MGG_01133-EcoR1-R	gcccttgctcaccatgaattcTCTCGATTTGCCCGAGTTAGG	Gene complementation
MGG_06434-UP-F	aagggaacaaaagctggtaccggaagcactttcgtctcctg	Gene deletion
MGG_06434-UP-R	tcagttaacgtcgacaagctttaaaggggttgctggatttg	Gene deletion
MGG_06434-DW-F	cgggaaccagttaacctgcagcgcaaacaaaacgagtctca	Gene deletion
MGG_06434-DW-R	cgctctagaactagtggatccgctgttgtgggtgttgaatg	Gene deletion
MGG_05748-UP-F	aagggaacaaaagctggtaccctcggggctaagtttgattg	Gene deletion
MGG_05748-UP-R	tcagttaacgtcgacaagcttactgcgcttgttccgaatag	Gene deletion
MGG_05748-DW-F	cgggaaccagttaacctgcagtggtgacgaatgtctgtggt	Gene deletion

MGG_05748-DW-R	cgctctagaactagtggatccggacatgtacggcaaggatt	Gene deletion
MGG_01130-UP-F	aagggaacaaaagctggtacctcacaccccagtccacacta	Gene deletion
MGG_01130-UP-R	tcagttaacgtcgacaagcttttctgcgcctgtttttgtaa	Gene deletion
MGG_01130-DW-F	cgggaaccagttaacctgcagccgcgatagatgatttggat	Gene deletion
MGG_01130-DW-R	cgctctagaactagtggatcctggagggaaatgaagtttgc	Gene deletion
MGG_08137-UP-F	aagggaacaaaagctggtaccaggagcagttcgagttgtgg	Gene deletion
MGG_08137-UP-R	tcagttaacgtcgacaagcttaaagcttgagaagcgaggaa	Gene deletion
MGG_08137-DW-F	cgggaaccagttaacctgcagggccggattttacaatgcta	Gene deletion
MGG_08137-DW-R	cgctctagaactagtggatcctggcgacaaaagacaaaaca	Gene deletion
MGG_14558-UP-F	aagggaacaaaagctggtaccATGTGCGTACCTATTGCAACCT	Gene deletion
MGG_14558-UP-R	tcagttaacgtcgacaagcttGGTACCGGTCACGATCATCATA	Gene deletion
MGG_14558-DW-F	cgggaaccagttaacctgcagAGGAAAGGAAAGTACTTGATGG	Gene deletion
MGG_14558-DW-R	cgctctagaactagtggatccAAGTCTTGCGGTAGTCGAGCTT	Gene deletion
pCB1532-MGG_14558-BamH1-F	cgctctagaactagtggatccACAGCCAACATCATGCAAGACA	Gene complementation
pCB1532-MGG_14558-EcoR1-R	gcccttgctcaccatgaattcTCGCCCGTATCGATCCCG	Gene complementation
MGG_00138-XbaI-F	tacccaagcatccaatctagaATGCTCAAGAAGAAAGGCGCC	Protein localization
MGG_00138-EcoRI-R	gcccttgctcaccatgaattcACCACCAATCCCAACAAATCG	Protein localization
MGG_01426-XbaI-F	tacccaagcatccaatctagaATGCCTGTCGTCAAAGGAGGG	Protein localization
MGG_01426-EcoRI-R	gcccttgctcaccatgaattcGTGGTACCCATTAGTAACCACAG	Protein localization
MGG_08985-XbaI-F	tacccaagcatccaatctagaATGACTTCACTCGACGTCCGC	Protein localization
MGG_08985-EcoRI-R	gcccttgctcaccatgaattcACGTTTCTGTCTCTTGCCCTTG	Protein localization
MGG_08137-XbaI-F	tacccaagcatccaatctagaATGGCCCCCGGCAAGGAC	Protein localization
MGG_08137-EcoRI-R	gcccttgctcaccatgaattcTGCTTCGCCTCCAACCTTG	Protein localization
MGG_03899-XbaI-F	tacccaagcatccaatctagaATGGCTGAGATGTCGCTAGGC	Protein localization
MGG_03899-EcoRI-R	gcccttgctcaccatgaattcCCCGGTTGCTTTGGCAAG	Protein localization
MGG_06434-XbaI-F	tacccaagcatccaatctagaATGAAGTGGATGCGGACAGACT	Protein localization
MGG_06434-EcoRI-R	gcccttgctcaccatgaattcTTCGGCAGGCCTTCCAGG	Protein localization
MGG_05099-XbaI-F	tacccaagcatccaatctagaATGGGTGTCATACGGAAAAAGACA	Protein localization
MGG_05099-EcoRI-R	gcccttgctcaccatgaattcAGCCTTGCCAACCCATCC	Protein localization
MGG_06898-XbaI-F	tacccaagcatccaatctagaATGACTCTACCCATTTCGCCAA	Protein localization
MGG_06898-EcoRI-R	gcccttgctcaccatgaattcGTTCATGATGGAGGCGATCG	Protein localization
MGG_05945-XbaI-F	tacccaagcatccaatctagaATGCCCAAAATCACGCGA	Protein localization
MGG_05945-EcoRI-R	gcccttgctcaccatgaattcGACGCCGTGGTGTCCAGA	Protein localization
MGG_05240-XbaI-F	tacccaagcatccaatctagaATGAGCAGCCACTCGGGG	Protein localization
MGG_05240-EcoRI-R	gcccttgctcaccatgaattcTAAGGGACTTCCAAGTGGATGTC	Protein localization

MGG_06120-XbaI-F	tacccaagcatccaatctagaATGGCATCAAGATGGAATCTTCG	Protein localization
MGG_06120-EcoRI-R	gcccttgctcaccatgaattcCAAGGGTAGGAGATCCTCAACTGC	Protein localization
MGG_01130-XbaI-F	tacccaagcatccaatctagaATGTCTCCGATGCACATGAGC	Protein localization
MGG_01130-EcoRI-R	gcccttgctcaccatgaattcTGCGCCAACCCTTTCCTC	Protein localization
MGG_05748-XbaI-F	tacccaagcatccaatctagaATGCTTCTCCCCTCTGCAGTC	Protein localization
MGG_05748-EcoRI-R	gcccttgctcaccatgaattcCCTGGACTTTGCTAGACGAGCT	Protein localization
MGG_01720-F	cttgaccgtctggcctttag	RT-qPCR
MGG_01720-R	tggtcacatcttgtgccatt	RT-qPCR
MGG_01012-F	ccaaagaggtcaaacccaaa	RT-qPCR
MGG_01012-R	ccttgcggtagaaagcagtc	RT-qPCR
MGG_00138-F	cagcgcaagactccacagta	RT-qPCR
MGG_00138-R	atgctcgtgattgagcctct	RT-qPCR
MGG_01426-F	gagagggagagctggaggat	RT-qPCR
MGG_01426-R	cgagtaagagccaaccaagc	RT-qPCR
MGG_08095-F	gtttcattccacgaccgact	RT-qPCR
MGG_08095-R	ttcgtaatacgctgctgctg	RT-qPCR
MGG_08137-F	acgtcaccaacgctttctct	RT-qPCR
MGG_08137-R	tcgtttacgacgatgctgag	RT-qPCR
MGG_02746-F	gcagctaccacttcgcctac	RT-qPCR
MGG_02746-R	gtgttccggctgagaatcat	RT-qPCR
MGG_03899-F	gccaagaacgggatatctga	RT-qPCR
MGG_03899-R	ctgctgccttgtccttatcc	RT-qPCR
MGG_10426-F	ggatgtcgcagtttgaggtt	RT-qPCR
MGG_10426-R	tcgcggaggtcttctaggta	RT-qPCR
MGG_06434-F	tgtttgaccctgagatgcag	RT-qPCR
MGG_06434-R	cagtgcgcgactcatagaaa	RT-qPCR
MGG_05099-F	tcttgatcagaccccagacc	RT-qPCR
MGG_05099-R	tccttgagcaactgctcctt	RT-qPCR
MGG_06898-F	gacacctgcctccaattgtt	RT-qPCR
MGG_06898-R	ctcgtgatgcgctttgtcta	RT-qPCR
MGG_05945-F	actcgagcgcagtttacgat	RT-qPCR
MGG_05945-R	gcactgatacctgcagacga	RT-qPCR
MGG_05240-F	caaagacccagaggaccaaa	RT-qPCR
MGG_05240-R	gacctcccagggaagaactc	RT-qPCR
MGG_06120-F	gacggttgagactggtggtt	RT-qPCR

MGG_06120-R	aagtctgcgctccacttcat	RT-qPCR
MGG_01130-F	ccatgaatctcgttccgtct	RT-qPCR
MGG_01130-R	ctgttggctgacatgatgct	RT-qPCR
MGG_01133-F	gctgaagagcacatgctgaa	RT-qPCR
MGG_01133-R	gcttcttcacactcccttcg	RT-qPCR
MGG_05748-F	aacaacaacaacggccaact	RT-qPCR
MGG_05748-R	tttgtggtgcttttgctgtc	RT-qPCR
MGG_14558-F	tcgatagagcatcccgtacc	RT-qPCR
MGG_14558-R	atctggtgaattgggtctcg	RT-qPCR
MGG_00138-TZ-F	ACAGTGGCACGAGAGGTGGT	Southern blot probe
MGG_00138-TZ-R	CGCATGTAGTCGAAGAGATAGAT	Southern blot probe
MGG_01012-TZ-F	gactttcgggacaagatgga	Southern blot probe
MGG_01012-TZ-R	acacccatcgcgaatagaac	Southern blot probe
MG01130-TZ-F	tctgcacgttgcgtaggtag	Southern blot probe
MG01130-TZ-R	cgtcctcagggttttgacat	Southern blot probe
MGG_01133-TZ-F	tctgcacgttgcgtaggtag	Southern blot probe
MGG_01133-TZ-R	cgtcctcagggttttgacat	Southern blot probe
MGG_01426-TZ-F	cgcgtttcttcaaagactcc	Southern blot probe
MGG_01426-TZ-R	aaagtggggacaaacgtcac	Southern blot probe
MGG_01720-TZ-F	TGTTGGAAAGAGCGGGAGCA	Southern blot probe
MGG_01720-TZ-R	AAGCGTGGATTGGCGAGATA	Southern blot probe
MGG_02746-TZ-F	GCCAAGCGGGACCTTACAAT	Southern blot probe
MGG_02746-TZ-R	GGAGGAGCCATCACGAGAATA	Southern blot probe
MGG_05099-TZ-F	AAGTGGGCTGGATGTTGTTT	Southern blot probe
MGG_05099-TZ-R	CTTGGTAGTCGTGTAGCTGTTTAA	Southern blot probe
MGG_05240-TZ-F	gcagcatgtgtcgatgattt	Southern blot probe
MGG_05240-TZ-R	actgtttacgaggcgaagga	Southern blot probe
MGG_05945-TZ-F	ctcttggatgaccacccact	Southern blot probe
MGG_05945-TZ-R	caaatgaaaggggtttcacg	Southern blot probe
MGG_08095-TZ-F	GAGTAGAACAAAGTTGAAAAGAGCG	Southern blot probe
MGG_08095-TZ-R	CTGGGGAGTAATTGGGAGGA	Southern blot probe
MGG_10426-TZ-F	gacgatgacgacgaagatca	Southern blot probe
MGG_10426-TZ-R	gtctttgccaagaaggcaag	Southern blot probe
MGG_14558-TZ-F	TGCGTGTTTAGAGCTTGTGC	Southern blot probe
MGG_14558-TZ-R	ATTGGCGTGCCTTTTGGT	Southern blot probe

Table S2

	Myb	Deleted	MY	Con	8hpi	24hpi	48hpi	72hpi	96hpi	Profile			
MGG_01720	Myb17	0	0.29377	2.42739	0.87019	0.43711	2.6996	1.5613	1.12981		48-96HPI and MY		
MGG_00138	Myb16	X	0.26869	3.17626	0.40819	0.69448	4.62889	1.88862	1.59181				
MGG_15357	Myb12	0	0.11866	4.32665	0.50869	0.39091	1.63571	1.67785	1.49131				
MGG_10426	Myb2	X	0.13445	2.89151	0.53407	0.29494	2.832	0.87167	1.46593				
MGG_01012	Myb15	X	0.15935	2.26624	0.7686	0.41188	1.68994	1.141	1.2314				
MGG_01426	Myb4	X	0.05159	1.40114	0.1297	0.21713	0.86051	0.74395	1.8703		Conidia late (formation)		
MGG_01133	Myb5	X	0.10831	5.86972	0.12101	0.09898	0.65065	0.8766	1.87899				
MGG_01130	Myb6	X	0.08542	0.17164	0.18395	0.54365	1.80768	0.4777	1.81605				
MGG_05748	Myb10	X	0.14046	6.18289	0.67901	0.63356	0.66202	0.41418	1.32099				
MGG_05240	Myb9	X	0.03941	0.3715	0.82057	1.73475	1.53485	1.02202	1.17943		24HPI		
MGG_06120	Myb19	0	0.23444	0.42749	0.66767	1.90164	0.62877	0.72898	1.33233				
MGG_08095	Myb9	X	0.36388	1.46227	1.18499	0.7764	0.5427	0.47904	0.81501		Little regulation		
MGG_05099	Myb12	X	0.20749	1.79146	1.05538	0.33089	0.2874	0.60759	0.94462				
MGG_03899	Myb14	X	0.08897	1.09643	1.66564	0.22732	0.33903	0.14622	0.33436		8HPI		
MGG_06898	Myb1	X	0.00636	0.37845	1.96182	0.83833	0.0172	0.02004	0.03818				
MGG_02746	Myb7	0	0.19945	2.77815	1.59925	0.27626	0.07351	0.3101	0.40075				
MGG_08137	Myb3	X	0.08723	0.8337	1.36378	0.8053	0.23667	0.5252	0.63622				
MGG_05945	Myb8	X	0.02566	0.07209	1.07608	1.00636	0.14351	0.52577	0.92392				
MGG_14558	Myb13	X	0.10274	2.97662	1.23138	0.68951	0.91194	0.45073	0.76862				

Table S3

Sequences producing significant alignments with more than 70 percent cover:

Sequences	Description	Scientific Name	Max Score	Total Score	Query Cover	E value	Per. Ident	Acc. Len	Accession
Select seq ref|XP_003709785.1|	uncharacterized protein MGG_14558 [Pyricularia oryzae 70-15]	Pyricularia oryzae 70-15	4526	4526	100%	0	100.00%	2305	XP_003709785.1
Select seq gb|ELQ36651.1|	hypothetical protein OOU_Y34scaffold00649g34 [Pyricularia oryzae Y34]	Pyricularia oryzae Y34	4510	4510	100%	0	99.91%	2615	ELQ36651.1
Select seq gb|QBZ54440.1|	hypothetical protein PoMZ_10140 [Pyricularia oryzae]	Pyricularia oryzae	4444	4444	100%	0	98.11%	2632	QBZ54440.1
Select seq gb|ELQ68318.1|	hypothetical protein OOW_P131scaffold00255g20 [Pyricularia oryzae P131]	Pyricularia oryzae P131	4404	4404	100%	0	97.87%	2571	ELQ68318.1
Select seq gb|ROW02559.1|	hypothetical protein VPNG_07863 [Cytospora leucostoma]	Cytospora leucostoma	555	681	90%	7.00E-158	37.34%	2285	ROW02559.1
Select seq gb|KUI62100.1|	hypothetical protein VP1G_09221 [Valsa mali var. pyri]	Valsa mali var. pyri	530	659	86%	2.00E-149	36.63%	2284	KUI62100.1
Select seq gb|OIW27663.1|	hypothetical protein CONLIGDRAFT_682689 [Coniochaeta ligniaria NRRL 30616]	Coniochaeta ligniaria NRRL 30616	614	723	82%	5.00E-178	39.22%	2253	OIW27663.1
Select seq gb|KAB5585523.1|	hypothetical protein GE09DRAFT_29357 [Coniochaeta sp. 2T2.1]	Coniochaeta sp. 2T2.1	579	690	78%	4.00E-166	38.69%	2211	KAB5585523.1
Select seq gb|KAA8631205.1|	hypothetical protein SMACR_04153 [Sordaria macrospora]	Sordaria macrospora	506	782	78%	3.00E-141	43.08%	2610	KAA8631205.1
Select seq gb|KAH7635984.1|	hypothetical protein B0T09DRAFT_31245 [Sordaria sp. MPI-SDFR-AT-0083]	Sordaria sp. MPI-SDFR-AT-0083	506	781	78%	5.00E-141	42.98%	2687	KAH7635984.1
Select seq gb|TRX97365.1|	hypothetical protein FHL15_001643 [Xylaria flabelliformis]	Xylaria flabelliformis	535	609	77%	4.00E-152	36.34%	2024	TRX97365.1
Select seq gb|RYP84680.1|	hypothetical protein DL769_001114 [Monosporascus sp. CRB-8-3]	Monosporascus sp. CRB-8-3	604	664	76%	7.00E-176	37.46%	2020	RYP84680.1
Select seq gb|RYP88518.1|	hypothetical protein DL770_004599 [Monosporascus sp. CRB-9-2]	Monosporascus sp. CRB-9-2	598	652	76%	2.00E-173	36.53%	2035	RYP88518.1
Select seq ref|XP_030990550.1|	uncharacterized protein E0L32_009657 [Phialemoniopsis curvata]	Phialemoniopsis curvata	531	934	75%	5.00E-151	42.68%	2017	XP_030990550.1
Select seq ref|XP_024511445.1|	uncharacterized protein SMAC_04153 [Sordaria macrospora k-hell]	Sordaria macrospora k-hell	508	780	73%	1.00E-141	43.08%	2675	XP_024511445.1
Select seq gb|KAH6848250.1|	hypothetical protein B0I37DRAFT_159719 [Chaetomium sp. MPI-CAGE-AT-0009]	Chaetomium sp. MPI-CAGE-AT-0009	509	768	72%	2.00E-143	40.27%	2000	KAH6848250.1
Select seq gb|RYP04937.1|	hypothetical protein DL764_004149 [Monosporascus ibericus]	Monosporascus ibericus	484	692	71%	3.00E-135	40.63%	2014	RYP04937.1